1-1-2014

Determination of Interior Vibration Levels from Tire/Wheel Assembly Non-Uniformities using a Monte Carlo Process

Rachel Wood Wheeler

Determination of interior vibration levels from tire/wheel assembly non-uniformities using a Monte Carlo process

By

Rachel Wood Wheeler

A Dissertation
Submitted to the Faculty of
Mississippi State University
in Partial Fulfillment of the Requirements
for the Degree of Doctorate of Philosophy
in Engineering
in the Department of Mechanical Engineering

Mississippi State, Mississippi

August 2014

Determination of interior vibration levels from tire/wheel assembly non-uniformities

using a Monte Carlo process

By

Rachel Wood Wheeler

Approved:

_____

Youssef Hammi
(Major Professor)

_____

Mohamad Qatu
(Minor Professor)

_____

Clayton T. Walden
(Committee Member)

_____

Mark F. Horstemeyer
(Committee Member)

_____

Kalyan K. Srinivasan
(Graduate Coordinator)

_____

Jason M. Keith
Dean
Bagley College of Engineering

Name: Rachel Wood Wheeler

Date of Degree: August 16, 2014

Institution: Mississippi State University

Major Field: Engineering

Major Professor: Youssef Hammi

Title of Study: Determination of interior vibration levels from tire/wheel assembly non-uniformities using a Monte Carlo process

Pages in Study: 84

Candidate for Degree of Doctorate of Philosophy

Variations in vehicle noise, vibration and harshness (NVH) response from one vehicle to the next can have significant impact on an automotive company's profile and profitability. The warranty claims due to excessive NVH response end up costing the manufacturers a large sum of money each year. In addition, the OEM will suffer a larger financial loss due to the poor perception of quality and customer dissatisfaction with their products due to the unacceptable NVH response. Therefore, measures must be taken to ensure less warranty claims and higher levels of customer satisfaction.

This research focuses on aspects of design variations that are costly or difficult to be avoided in the design process such as variations with rubber parts and variations due to rotating components. Vibrations induced at the tire/wheel assembly due to variations in the radial and tangential forces and radial runout are responsible for the driver-felt vibrations that can lead to a large number of warranty claims. The purpose of this research is to improve the process of determining and analyzing vibration sources in the tire/wheel assembly in order to benefit the automotive manufacturer during the development and manufacturing phases. This research identifies the relationship between

non-uniformity forces of the tire/wheel assemblies and the driver-felt vibrations during typical highway driving speeds. The contribution from each assembly location is analyzed and sensitivities are determined. A Monte Carlo process is used to predict numerous non-uniformity properties that are statistically representative of the assembly properties that can be expected at the manufacturing plant. The Monte Carlo produced non-uniformity properties are combined with the sensitivities to predict driver-felt vibrations that can be expected from vehicles leaving the manufacturing plant. This process provides the tools to determine an acceptable level of non-uniformities based on targets for interior vibration levels or determine if the vehicle sensitivities to non-uniformities need to be improved.

DEDICATION

The traditional wedding anniversary gift for the first year of marriage is paper. So I dedicate this *paper* to my husband Chase. My most faithful fan. My strongest supporter. This first year of marriage has been better than I ever imagined, and I can't wait to experience this next chapter with you. I love you more.

ACKNOWLEDGEMENTS

None of this would be possible without the guidance, support, and patience of my committee members: Dr. Qatu, Dr. Hammi, Dr. Walden, Dr. Horstemeyer, and Dr. King. Thank you for believing in me.

I would like to acknowledge the Center for Advanced Vehicular Systems (CAVS), the Bagley College of Engineering Fellowship Program, and the NASA/Mississippi Space Grant Consortium for funding throughout my time in graduate school.

TABLE OF CONTENTS

LIST OF TABLES

LIST OF FIGURES

CHAPTER I

INTRODUCTION

Background

Variations in vehicle noise, vibration and harshness (NVH) response from one vehicle to the next can have significant impact on an automotive company's profile and profitability. Variation can be caused by variability in design (e.g., tolerance stack up), material (e.g., stiffness properties), manufacturing (e.g., locations of parts in assembly, welding), customer usage, environmental conditions, or other sources. Such variation in the vehicle response causes a higher percentage of produced vehicles to go out of specification in terms of their NVH response. This is found to be a major component of warranty claims. There is evidence that more than one fourth of warranty claims for a typical original equipment manufacturer (OEM) are first detected through excessive noise and vibration levels. In addition, variations in vehicle NVH response can cause a loss in customer satisfaction. The warranty claims due to excessive NVH response end up costing the manufacturers a large sum of money each year. In addition, the OEM will suffer a larger financial loss due to the poor perception of quality and customer dissatisfaction with their products due to the unacceptable NVH response.

Measures must be taken to ensure less warranty claims and higher levels of customer satisfaction. Excessive variations in vehicle response cause manufacturers to consider lowering the target mean value so that fewer vehicles can exceed the

specification limit. This approach is found to be costly in terms of warranty claims, program quality, and customer satisfaction. In addition, it does not guaranty satisfactory results if a high level of variation is encountered. Instead, research has to be performed to understand the root cause of variation and control it. As a result, OEMs have implemented design for variation in the vehicle design process to secure a response that is within vehicle specification.

This research focuses on aspects of design variations that are costly or difficult to be avoided in the design process. In particular, certain materials (e.g. rubber) are known to have variation that is either unavoidable or proven costly if tighter control is desired. Manufactured rubber stiffness can vary up to +/- 10% of the mean value. Rubber materials are used as engine mounts, subframe mounts, exhaust hangers, and tires, as well as other components. In other examples, variations due to imbalance in rotating components can also be unavoidable or costly to control. Some of the major components in the vehicle that are known to have imbalance, and traditionally cause NVH issues and concerns include the crankshaft, drivetrain components, and wheels. The purpose of this research is to assess some of the sources of variations in the tire/wheel assembly and the methods used in the literature to design a more robust system to such variations.

This project focuses on improving the process of determining and analyzing vibration sources to benefit the automotive manufacturer during the development and manufacturing phases. The following review provides a summary of the research and information available relating the testing and understanding of vibration phenomena to the automobile industry.

Technical Approach

The general NVH approach is that noise and vibration energy is born at a source. In almost all the cases studied, the source is a structural or machine element. The noise and/or vibration energy is then transferred through the vehicle structure and enclosures (or vehicle exterior like surrounding air) to a receiving point. This is called the path. The receiving point (a customer touch point) is often referred to as the receiver. If the path includes an energy transfer through air, the NVH energy is referred to as airborne. Although we refer to this as airborne noise, the actual energy was born at a structure (e.g. the housing transmitting such energy in the case of transmission whine). If the NVH energy is going through a structural path, the NVH concern is referred to as structureborne. In general, structureborne noise and vibration concerns are of low frequency nature. This is the case because of two reasons: higher frequency energy is usually damped in the path, and customers are less sensitive to vibration energy at higher frequencies.

Wheel-induced vibration can be felt by the customer at many customer touch points (CTPs). The ones that are typically considered include:

a. Vibration at the steering wheel. It is usually observed as steering shake or steering nibble (shimmy).

b. Vibration in the seat. It should be noted here that this particular assessment may require the acceleration to be measured in all three directions. This may be a cause of unacceptable levels of vibrations under cruising conditions.

c. Vibration in the accelerator pedal.

Sound or noise can be measured at the driver's out-board ear, drivers in-board ear or both. There are other CTPs. One can consider the floor pan or seat track of other seats in the vehicle, sound measurements of other passenger locations, or other types of measurements. Most vehicles when driven in the North American market have only the driver, so these other considerations will not be investigated or included in the scope here.

A cross-functional approach involving both manufacturing and design/development is adopted. Priorities are determined based upon a detailed review of the current three months in service (3MIS) warranty data as well as input of customer satisfaction teams (CST) for a typical car manufacturer. This is reviewed, and the current direction for conducting research is on a midsize car. This is chosen because of its production volume, production location, and potential impact to warranty.

A diagram that relates the warranty claim generally referred to as "vehicle vibrates while driving", as perceived by the customer, to design parameters is shown in Figure 1. The figure shows how this issue has to first be translated to values measured objectively at customer touch points (seat track, steering wheel and possibly others). While this seems to be a trivial step, experience shows that it may actually be a demanding one. Challenges may rise in trying to duplicate the customer complaints both at the dealer with the actual vehicle in which the customer experienced the concern or in a similar setting with a similar vehicle. The second challenge is to find the actual metric that can be used for measurement and location. The third is to determine the levels at which such measurements become a customer complaint either leading to a warranty claim or loss of customer satisfaction, or both.

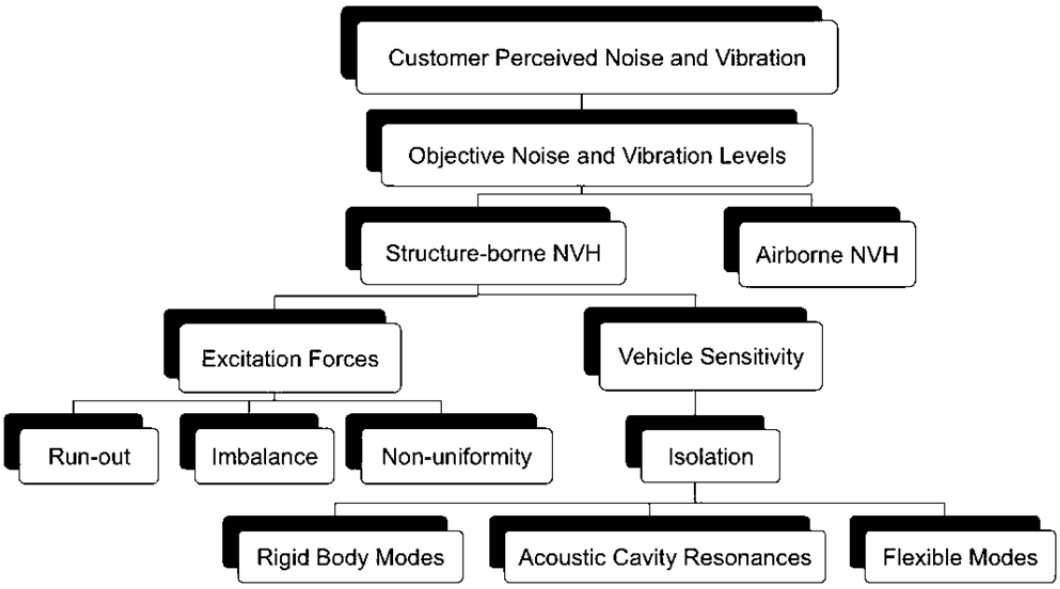

Figure 1 Tire/Wheel NVH Cascade Summary and Possible Design Parameters

The quality of the ride in a vehicle is affected by the tires in two ways [3]. Harshness is the first, and it refers to the vibration that is created from the tire rolling over an irregular road surface. The second way that tires affect the ride quality of vehicles is through non-uniformities of the tires. Non-uniformities contribute to vibrations that are felt when a vehicle is driven on a smooth road, because non-uniformity refers to structural irregularities within the tire itself. It is important to emphasize here the separation between wheel-induced vibrations and road-induced vibration. The proposed work will address in-vehicle NVH induced by the wheel assembly only. The wheel assembly will include the wheel and tire. NVH due to the brake systems will not be addressed here (thus, the brakes are assumed off). The brake system that is mounted on the wheel, however, will be included in the analysis as a part of the wheel. Sound measurements are not shown to be necessary for the problem we are investigating here

because of its low frequency. Figure 1 shows the in-vehicle NVH concerns when cascaded to its sources in the wheel assembly.

Before a detailed study is conducted on how to assess total vibration at CTPs, it is important to understand the vibration transfer mechanism from the wheel assembly to the vehicle's main frame. The vibration is induced at the wheel assembly. This can be due to many factors: wheel imbalance, tire uniformity, wheel alignment, run-out, as well as others (bad bearing, joints, half shafts, etc). The scope here is to study tire non-uniformity.

Non-Uniformity of Tires and Wheels

A rotating tire/wheel assembly produces 3 forces and 3 moments at the spindle that correspond to the 3 axes X, Y, and Z that are expected in a 3 dimensional problem [3]. These forces are referred to as radial force, lateral force, or tangential force. These forces are depicted in Figure 2. Of these 3 forces and 3 moments, only 2 forces and 1 moment are actually responsible for the majority of vibration energy that is transmitted to the driver. These are the radial and fore-aft (tangential) forces and the aligning moment. Force variations refer to the change in these forces as the tire rotates under a load. The force directions are described in Figure 2.

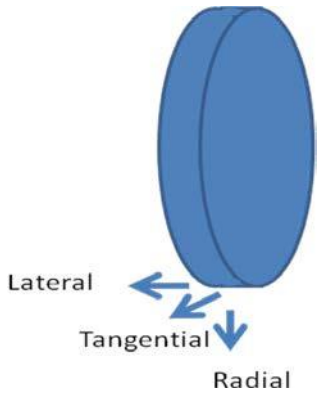

Figure 2 Non-Uniformity Force Directions Acting on the Tire

Radial Force

Variation in the radial force can be caused by out-of-roundness due to radial runout [3]. For a tire with constant stiffness in the radial direction, the radial force variation can be described using the equation below where k_R is stiffness in the radial direction and R_n is radial runout.

—— Eq. 1

The first harmonic of the radial force variation (RH1) is linearly correlated to the first harmonic geometric runout.

The radial force variation interacts with the first vertical flexural mode to produce significant energy at frequencies above about one half of the mode's natural frequencies [3]. At highway speeds, this interaction is significant for higher harmonics (greater than 2nd harmonic) but is not relevant for RH1 or RH2. Therefore, radial force variation does not show a major change with increasing speeds.

Fore-Aft Force

Rolling radius variation is the main cause of fore-aft force variation [4]. The fore-aft (or tangential) force is a function of variation in the tire's rolling radius (that varies due to radial runout) and can be described using the equation below [3].

Eq. 2

The fore-aft force is therefore proportional to the square of the rolling velocity and the inertia of the tire/wheel assembly. This relationship implies that higher fore-aft uniformity problems will result from larger rim diameters, heavier tire/wheel assemblies, and higher vehicle speeds. At speeds above 100 km/hr, the first harmonic of the tangential force variation (TFV1) becomes significant. All harmonics of tangential force variation are affected by the lower frequency torsional mode of the tire (first longitudinal mode).

Tread gauge variation is the difference in height of the tread blocks with respect to the belt surface [4]. These variations occur due to extrusion thickness variations in the tread and rubber splices. The TFV1 is relatively independent of tread gauge variation (TGV) [4]. However, the RH1 is strongly dependent on TGV as a part of the overall geometric surface runout. The technique of grinding is used to reduce the geometric non-uniformity of TGV and is therefore effective in reducing RH1 but not TFV1 [4].

Categories and Harmonics

Non-uniformities can be divided into 3 categories: stiffness, mass, and geometry non-uniformity [4]. The combination of these variations, along with phasing, leads to spindle force variations that are transmitted through the vehicle to be felt as vibrations by

the driver. Mass variations of the tire/wheel assembly are controlled by balancing in order to eliminate the effect that this non-uniformity has on ride quality [4]. Even though the effect is mitigated, the mass variation is not removed and the tire will still deform inconsistently during rolling. However, non-uniformities due to mass variation are not generally studied any further since their contribution to driver-felt vibrations can be controlled with proper tire/wheel balancing. Stiffness variations are also not studied any further since they are mostly caused by manufacturing discrepancies such as ply overlap, splices, or other geometric variations [4]. Generally, the geometric variations contribute more to non-uniformity than the stiffness variations that they cause. Belt runout and tread gauge variation along the circumference of the tire are types of geometric non-uniformities [4]. The dominant force generation mechanism is the angular acceleration caused by radial runout which is a geometric non-unifomity [4]. Radial runout variation is the change in distance of the center of the rolling assembly in reaction to the change in radius of the assembly at the road. This can be simplified as the same concept of a circular ring that is rotating off center. Angular acceleration is found by differentiating the angular velocity that is a function of runout. Angular acceleration due to rolling radius variation is proportional to the square of the average angular velocity, so it is the major mechanism of runout force generation. Radial runout of the mounted tire with respect to the spindle is the major component in both fore-aft and radial force first harmonic variations.

Variations can be expressed in peak-to-peak numbers. Variation is also described in tire order. There are variations in first order (referred to as first harmonic), second order, or higher orders. The tire and wheel manufacturers are responsible for the higher

order harmonics (greater than 2nd order) and therefore must identify and correct any excitations of these orders [3]. The vehicle manufacturers are responsible for designing the structural response of the vehicle to all harmonics of each force and moment created by rotation of the tire/wheel assembly. A customer makes tire/wheel assembly adjustments, such as balancing, in order to adjust the first order behavior only. First order non-uniformities contribute the most to the disturbances in the frequency range that correlate to driving speeds [4].

Correction Techniques

Every tire and every wheel have non-uniformities, and the assembly of the tire and wheel introduces even more non-uniformities due to the interaction of the forces between the two [5]. For simplification purposes, the assembly is assumed to have a summation of non-uniformities from the tire and wheel. This generalization is the reasoning behind the process of match mounting in which the tire and wheel are mounted so that the peak location of the first harmonic radial force of the tire is mounted with the first harmonic radial runout low spot of the wheel (or 180 degrees from the peak location of the first harmonic radial runout) in order to reduce the overall first harmonic runout of the assembly. Successful match mounting also reduces TFV1 (fore-aft or tangential first harmonic force) of the assembly at highway speeds. Match mounting is supposed to produce an assembly that has a maximum first harmonic radial force that is the difference between the radial force of the tire and wheel due to phase cancellation [5]. In reality, this value is always much less than what is expected and randomly distributed. The difference between the expected value and the radial assembly force is explained by the addition of

the interaction forces of the assembly. There are other implications on the second harmonics.

In another attempt to correct the first harmonic non-uniformity forces, manufacturers may apply the technique of uniformity grinding of the tires [3]. Uniformity grinding is the process of changing the tire's tread surface to reduce RH1 (first harmonic radial force variation) of the tire. This technique was widely used in the 1970's but is no longer popular due to the unsatisfactory appearance of the resulting tire and its ability to result in uneven wear. The addition of weights has also been investigated as a way to correct the first harmonic non-uniformity forces; however, this technique has proven unsuccessful [3].

Measurement

Uniformity is measured experimentally by applying a consistent force to a rotating tire and measuring the spindle force variations at low (e.g. 60 rpm) or high (e.g. 400 rpm) rolling speeds in the clockwise and counterclockwise rolling directions [4]. The measurement is taken in the time domain and a Fast Fourier Transform (FFT) is performed to report the first, second and possibly higher harmonics. These force variations are then decomposed into harmonics that relate to the revolutions of the tire. It is generally found that the first harmonics contribute the majority of the total level of non-uniformity. This test is done for sample tire/wheel assemblies in a typical assembly plant to make sure that it meets certain specifications (not to exceed upper limits for non-uniformity, imbalance, and/or run-out). The high speed uniformity tests, often using specialized equipment, are imperative due to the difficulty in predicting high speed

results from the low speed uniformity data since there is only a weak correlation between the two [4].

Vehicle Sensitivity

The transfer function of the vibration energy caused by the non-uniformity of the tire (and/or imbalance) to the CTPs can be measured experimentally. The difference in the NVH signature divided by the difference in non-uniformity is frequently referred to as vehicle sensitivity for non-uniformity [2]. For vibration acceleration signature, this will be measured in $(m/s^2)/N$. Vehicle sensitivity functions can be determined analytically by developing the transfer function from the tire/wheel assembly and the CTPs. The determinations of such transfer function can be made using existing models of the main frame of the vehicle and conducting a finite element analysis (FEA) on it. The experimental approach for determining the transfer function can be valuable to determine variations in the transfer function itself (part to part variation) as a result of possible variations in the parts of the main frame, welding or other sources. It is also useful to correlate the analytical model using FEA with experimental measurements. This is beyond the scope of this work.

In-Vehicle NVH Assessment

The total vibration at the CTPs is assessed as the product of the forcing function (non-uniformity measured in Newtons) and the transfer function (or vehicle sensitivity). This is to be done in the frequency domain.

Eq. 3

In the above equation, a_i refers to the acceleration (m/s^2) at a CTP (e.g. steering wheel nibble or shimmy) due to the non-uniformity and vehicle sensitivity of one tire/wheel assembly, as noted by the subscript i. The total acceleration is determined by adding all the acceleration values (i=1,2,3,4) coming from the non-uniformity of each of the four tire/wheel assemblies $(F)_i$ and the corresponding vehicle sensitivity function $(a/F)_i$. It should be noted again that due to part to part variations of vibration sources like non-uniformity and imbalance, and possibly vehicle sensitivity, a Monte Carlo process is used.

In a Monte-Carlo process simulation, the forcing function (e.g. non-uniformity) is generated randomly based on the statistical parameters gathered from measurements. In addition, the sensitivity function may be described as a deterministic function (one curve) or in a statistical sense. In practical settings, assessment of a sensitivity function for a reasonable population may not be affordable and often, one sensitivity function is used. This will be done in this research. In-vehicle assessment is made using Equation 3 for each of the generated numbers for the forcing function. All interior NVH assessments are then gathered and a statistical distribution is then described. The output of this will shed light on how many possible failures one would expect in a million (as an example). This is key for a design for six sigma (DFSS) approach. This will lead to software and optimization tools for the design engineer to determine the most appropriate approach to handle objectionable interior vibration levels induced by sources at the wheel assembly. This model will then be used to determine the forcing function's distribution (e.g. non-uniformity) that leads to acceptable six sigma performance for NVH. This gives the

engineer the choice of whether to request a more stringent control of the variations (e.g. uniformity) or design the system (i.e. the vehicle) to be robust to them (i.e. improve vehicle sensitivity). This research is to develop the computational tool to help the engineer decide the better approach (e.g. economically) to achieve acceptable interior NVH levels.

Challenges with Non-Uniformity Testing and Current Models

The automotive consumer expects a ride quality that depends on tire/wheel assemblies that have a high degree of uniformity. In reality, it is impossible to avoid non-uniformities of the tire/wheel assembly. Therefore, tire and automotive manufacturers must attempt to control and reduce the non-uniformities. A vital step in controlling the ride disturbances in a vehicle is to establish boundaries for tire and wheel uniformity. FTIRE is a physics-based tire model that uses force variations of tires and the model equations to predict geometric non-uniformities which lead to the measured spindle force variations that are transmitted through the vehicle to cause ride discomfort [4]. Low speed force measurements do not work well to predict the longitudinal force variations at highway speeds, so high speed uniformity tests are used even though they are more expensive and time consuming [4]. Simulations have shown a peak in steering wheel angular acceleration around 110 km/hr or 13 Hz, but no difference between the right or left front tire. Similarly, there are no non-uniformity induced steering wheel accelerations when moving the tire to the rear positions according to the FTIRE model [4].

The forces of the assembly can be measured directly, but measuring the forces for the tire and wheel separately is more difficult [5]. The tire forces are measured after mounting it on a perfect wheel where there would be no interaction forces and no effects

from the wheel. The wheel forces cannot be measured so the geometric wheel runout data is measured, and the forces are then estimated by multiplying the runout data by the tire stiffness. This adds to the difficulty in measuring and analyzing the pieces of the tire/wheel assembly separately.

This research will investigate the relationships between the customer-felt vibrations and the location of the tire/wheel assembly with non-uniformity. Sensitivities of all 4 assembly locations will be more accurately measured using the high-speed uniformity testing that provides information that better relates to the highway driving speeds where the vibration complaints generally occur.

Summary

A detailed procedure is described for in-vehicle NVH assessment as a result of tire/wheel assembly non-uniformities. Vehicle sensitivity is found experimentally (to incorporate variations). Total in-vehicle response is then found in a statistical sense as a result of the statistical data for non-uniformity added from all the wheels. A program is needed to help the engineer make the better decision of whether to request tighter control for tire uniformity or implement vehicle design changes to improve sensitivity.

CHAPTER II

EXPERIMENTATION

In order to investigate the role that tire/wheel non-uniformity plays in driver-felt vibrations, the tire/wheel assemblies are to be the independent variable. A vehicle with tire/wheel assemblies with low and known values for non-uniformity is tested for interior NVH levels. A tire/wheel assembly with known, higher values for non-uniformity is then placed in each of the four locations of the vehicle: front driver side (FD), front passenger side (FP), rear driver side (RD), and rear passenger side (RP). Measurements are taken for each of the four set-ups. Four sensitivity curves are then determined for each of the tire/wheel assembly locations.

Equipment

Sedan general specifications

- 2.5 Liter Inline 4 Cylinder Engine
- Continuously Variable-Speed Automatic Transmission
- 175 hp @ 5600 rpm
- 180 ft-lbs. @ 3900 rpm
- Front Wheel Drive
- 9 ft. 1.3 in. Wheel Base
- 3180 lbs. Curb Weight

- Four-Wheel Independent Suspension
- MacPherson Strut Front Suspension
- Multi-Link Rear Suspension
- 16 x 7.0 in. Aluminum Wheels
- P215/60R T Tires

For this experiment, the sedan was fitted with triaxial accelerometers to measure the vibrations near the front wheels to serve as a baseline and control. This baseline was used to make sure that the accelerometers at the customer touch points (CTPs) would not be overloaded during the road tests and to quickly recognize a problem with the vehicle that could possibly cause inaccurate data at the CTPs. Triaxial accelerometers were also used to measure the vibrations at some of the CTPs including the steering wheel and seat track. A single axis accelerometer was also mounted on the accelerator pedal. The accelerometers have a related uncertainty of 2% for the frequency and temperature range in question. Rare earth magnets and dental epoxy were used to secure the accelerometers so that the sensors remained in similar orientations for the duration of the testing and to minimize any vibration interaction between the sensor and the mounting location. An additional channel of the data acquisition equipment was connected to the on-board diagnostics plug of the vehicle to acquire the CAN-bus data for the rotational speeds of the wheels. This information was used to determine and report the vibration data related to the first and second harmonics of the tire/wheel assemblies.

Five tire/wheel assemblies were supplied for the testing: Set A (1A, 2A, 3A, 4A) and 2D. Set A consisted of 4 tire/wheel assemblies that passed the current manufacturing specifications, and was used as the baseline for the vibration testing. Overall, the

properties of assembly 2D were much higher than the Set A assemblies and in some cases exceeded the specification limits. Due to its high non-uniformity properties, assembly 2D was selected to be rotated to all positions on the vehicle in order to test the sensitivity of the vehicle. The following table shows the individual properties of the tire/wheel assemblies.

Table 1 Kokusai Data of Tire/Wheel Assemblies

				High Speed - RESULT data (Imbalance NOT included)					
				RFV (N)			TFV (N)		
Date	Assy type/size	Assy #	RRO1 (mm)	OA	RH1	RH2	OA	TFV1	TFV2
1/31/2011 14:20	16" Conti + Aluminum	1A	0.14	40.18	17.61	11.06	145.27	40.71	120.18
1/31/2011 14:58		2A	0.29	64.88	48.54	25.80	84.87	54.00	27.77
1/31/2011 15:11		3A	0.28	68.48	35.54	13.51	100.15	16.41	81.89
1/31/2011 15:29		4A	0.36	61.29	41.21	35.52	78.92	46.94	49.84
1/31/2011 13:51		2D	0.47	120.04	91.39	48.31	148.75	65.52	93.02

LMS TestLab 11A was used along with an LMS front end to acquire and analyze the vibration data collected during the test runs.

Testing Procedure

A portion of Highway 82 in Starkville, MS was selected as the testing location, and the left lane was used for each test run. The start of data acquisition occurred at the same spot for each test run. The vehicle was driven at a constant speed for the duration of each test, and the same person drove the vehicles for each test run. There were 5 different test speeds.

1. 90 km/hr
2. 100 km/hr
3. 110 km/hr
4. 115 km/hr
5. 120 km/hr

There were also 5 different test setups.

1. Vehicle with all Set A assemblies
2. Vehicle with assembly 2D in the FP position
3. Vehicle with assembly 2D in the RP position
4. Vehicle with assembly 2D in the FD position
5. Vehicle with assembly 2D in the RD position

LMS Test Lab was used to acquire the same set of data for each test run. Vibration levels were collected once every 0.8 seconds for a total of 300 seconds of the driving for both the first and second harmonics. This yielded a total of 375 data points for the first order vibration signature of each test run. The goal of the test is to find the maximum and average vibration levels. Due to phasing of the assemblies in relation to one another, the test needs to run for 300 seconds in order to witness between 3 and 7 phases [8]. Within the 300 second test, the high and low spots of the assemblies will eventually be in phase and directly out of phase with each other so that the maximum vibration levels due to these interactions will be measured and included in the resulting 375 data points. The rotational speeds of the wheels were recorded using the vehicle's CAN-bus data. Since the wheels were seen to rotate at slightly different speeds, it can be determined that multiple phases were witnessed during the test runs.

Since triaxial accelerometers were used at the steering wheel and seat track, the overall vibration levels at these CTPs had to be calculated using the sum of the squares technique to combine the X, Y, and Z components. The test data was smoothed in order to remove bumps that may have occurred due to abnormalities on the road. A value was selected to represent the allowed jump in vibration level between points. If that threshold was exceeded, the data point was replaced with the average of the ten surrounding data points. To further smooth the data, each data point was then replaced with the average of the 5 surrounding data points. The overall maximum and average values of the resulting data are selected and used for the remaining evaluations. The results are seen in the following graphs. All data are presented for the first order of the tire/wheel assembly.

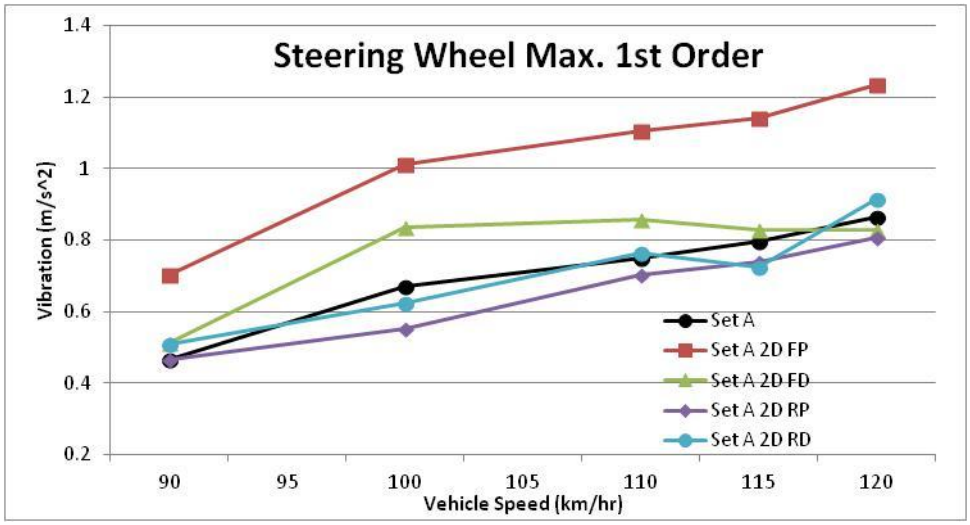

Figure 3 Maximum Vibration Levels at Steering Wheel

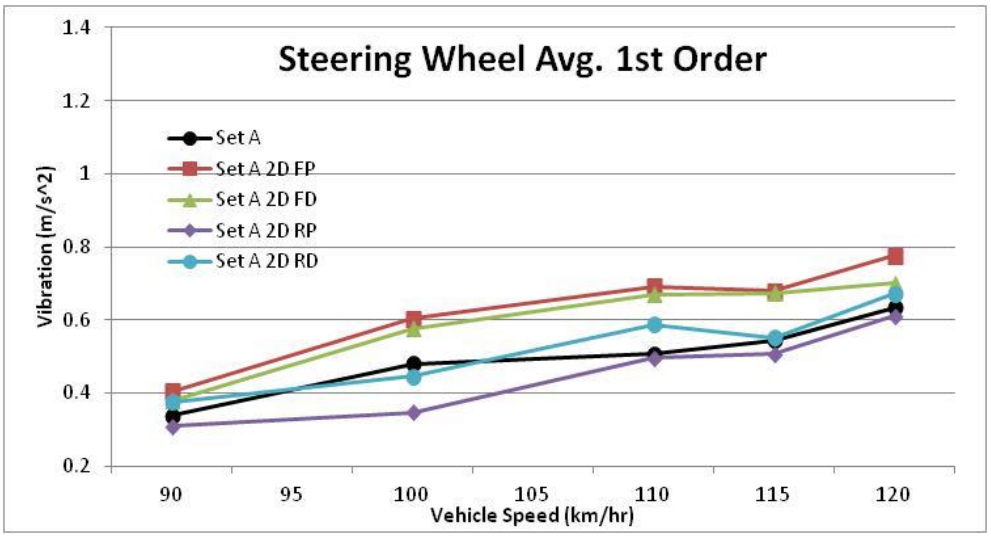

Figure 4 Average Vibration Levels at Steering Wheel

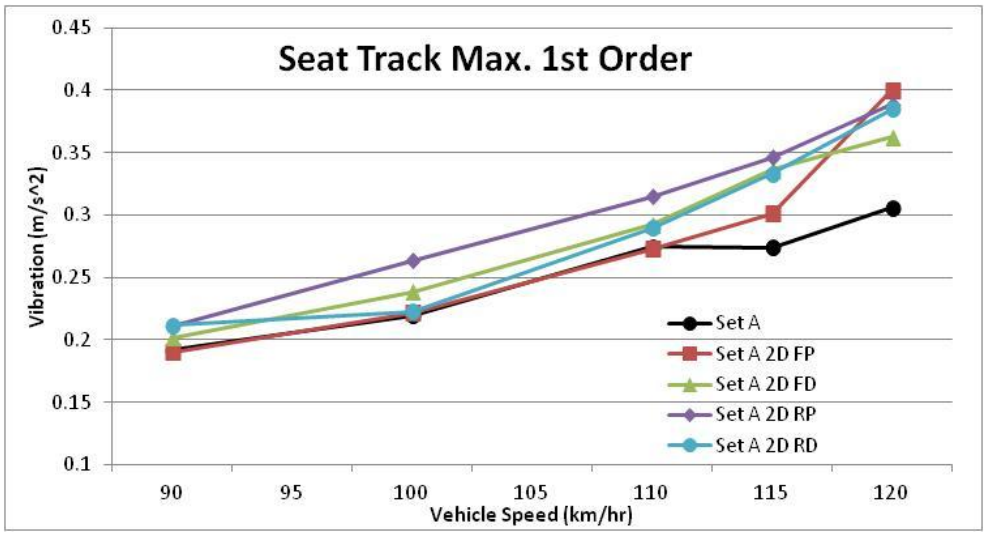

Figure 5 Maximum Vibration Levels at Seat Track

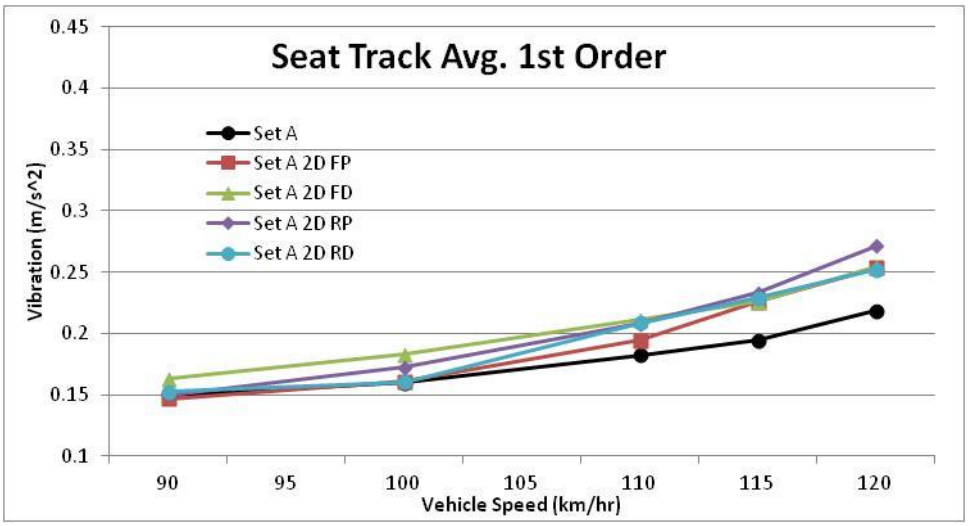

Figure 6 Average Vibration Levels at Seat Track

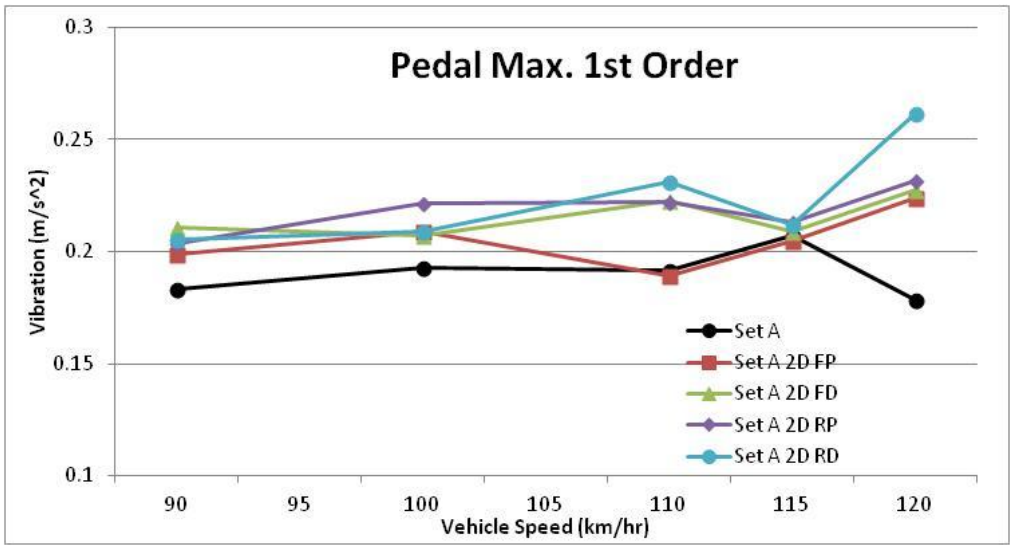

Figure 7 Maximum Vibration Levels at Pedal

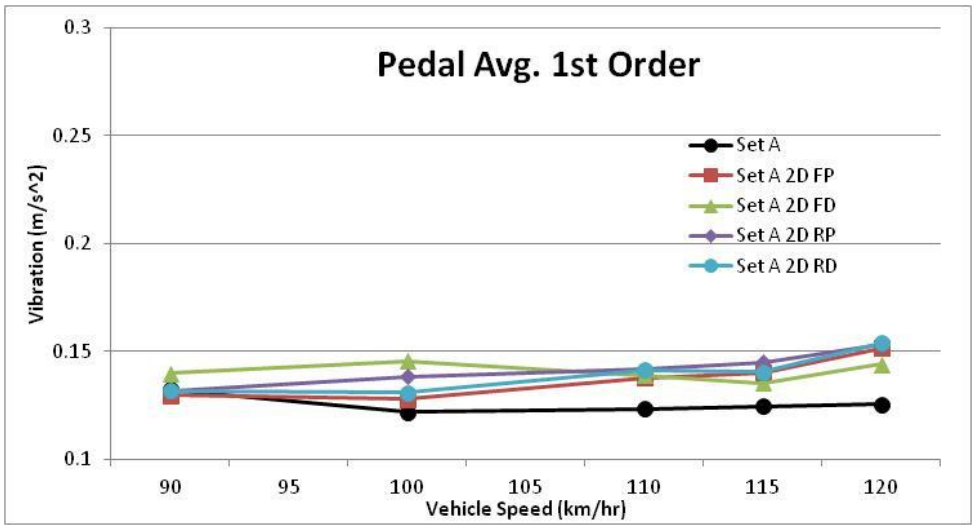

Figure 8 Average Vibration Levels at Pedal

For an added level of reliability, the test procedures were all repeated on a similar stretch of highway in the opposite direction. The selected peak acceleration from vibration values measured at the pedal were seen to vary by an average of 0.029 m/s^2 over the range of test speeds for each vehicle test setup. The variation in peak acceleration from vibration values at the seat track is 0.012 m/s^2 and at the steering wheel is 0.046 m/s^2. The selected average acceleration from vibration values measured at the pedal, seat track, and steering wheel varied by an average of 0.017, 0.005, and 0.025 m/s^2 respectively. The following 2 figures show a comparison of these test runs that were performed in the East and West directions. The small amount of variation can be seen between the two runs.

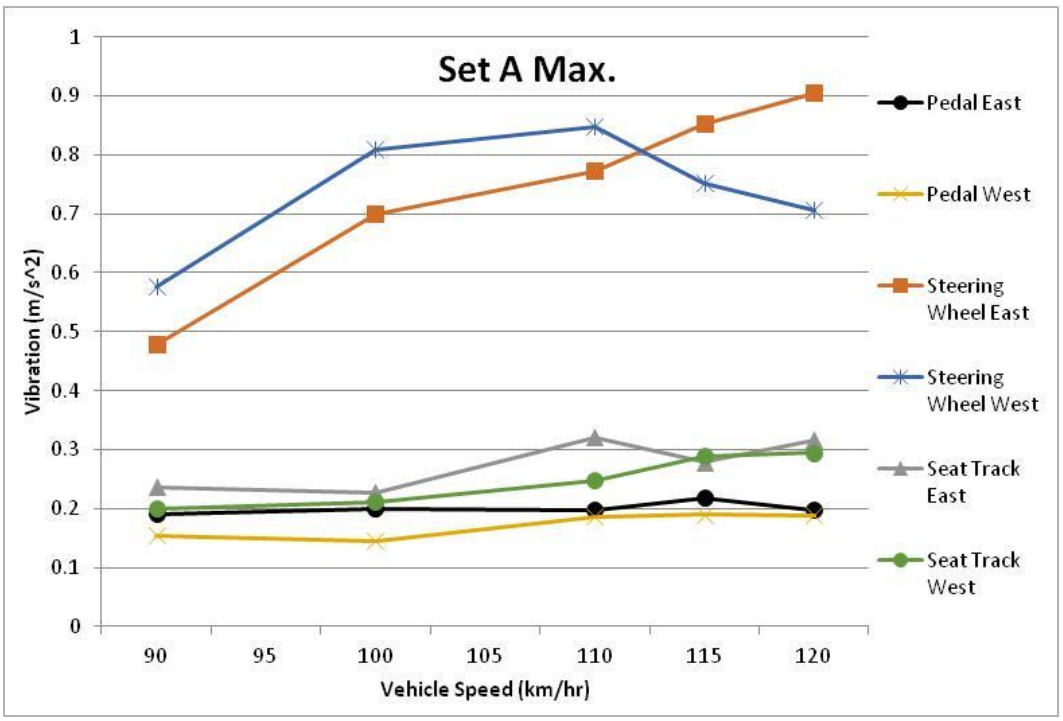

Figure 9 Comparison of maximum vibration acceleration values from East and West test runs

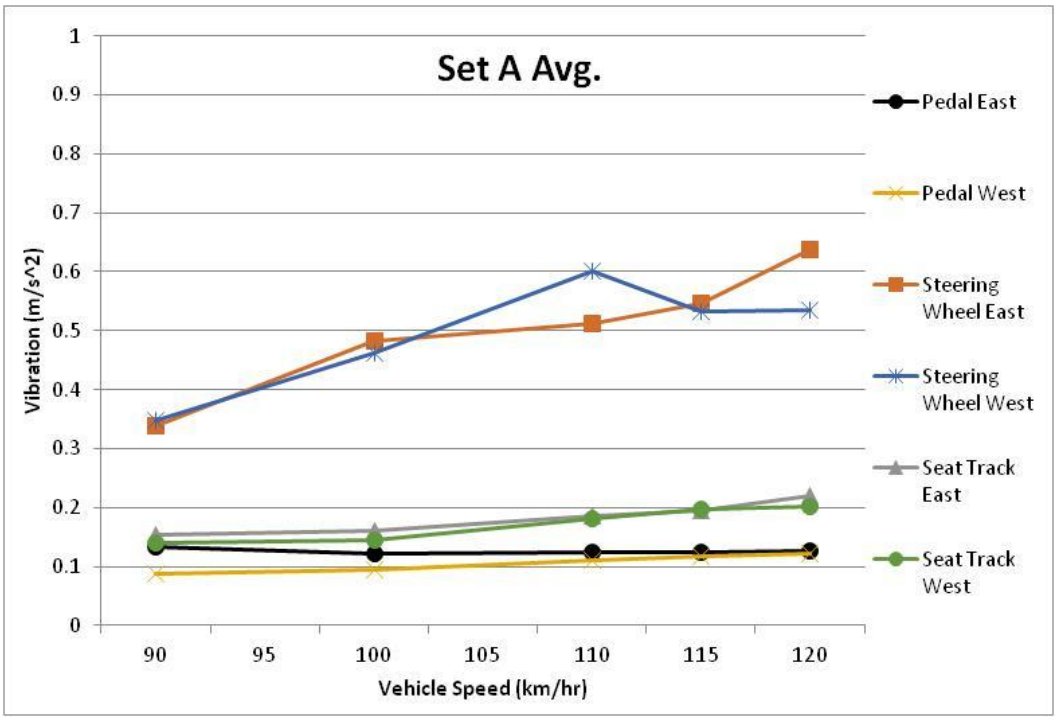

Figure 10 Comparison of average vibration acceleration values from East and West test runs

Sensitivity Calculations

Sensitivity calculations were made by finding the difference in vibration levels at each CTP for each assembly position divided by the difference in non-uniformity at each test speed. The non-uniformity information for 2D and Set A assemblies was provided from high-speed uniformity testing performed on a Kokusai machine. Using this high-speed data allows for more accurate sensitivity calculations since the properties were acquired at rotational speeds similar to the operating speeds seen during highway driving and the test procedure described in this research. Equation 4 was used to calculate these sensitivities at each frequency. The difference in vibration acceleration (V_{2D}-V_A) at each CTP is divided by the change in forcing function (FF_{2D}-FF_A), or non-uniformity in this

case. Sensitivities are calculated for each assembly position with the value of the denominator being dependent on the location of the assembly.

$$S = \frac{V_{2D} - V_A}{FF_{2D} - FF_A} \qquad \text{Eqn. 4}$$

Radial Force Variations

Sensitivities to changes in radial force variations (RFVs) at each assembly position for each CTP and test speed were evaluated using the Kokusai high-speed measurements for radial force variation without imbalance (meaning that the non-uniformity measurements will not be affected if the assemblies are balanced later). The summary of radial force variations for each assembly used in the testing is seen below along with the position of each Set A assembly.

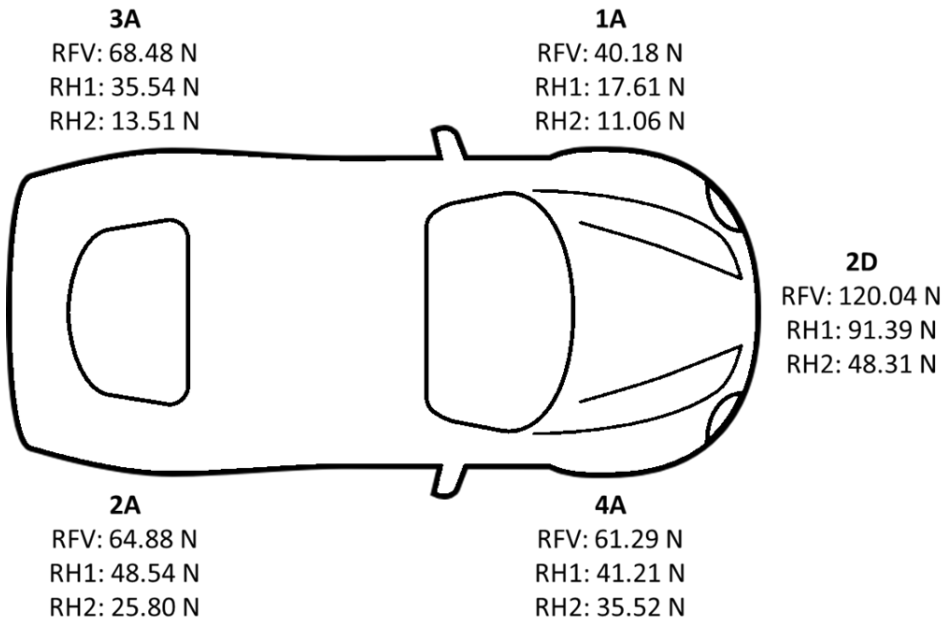

Figure 11 Radial Force Variations and Locations of Set A and 2D Assemblies

The sensitivities to radial force variations for each CTP and assembly position are calculated using both the maximum and average vibration recorded during the highway test runs. This produced two sensitivity curves for each force variation, CTP, and assembly position. These curves were averaged at each test speed to produce the following sensitivity curves over angular velocity of the wheels (cycles/second) relating to the first order of the test speed range of 90 to 120 kilometers per hour.

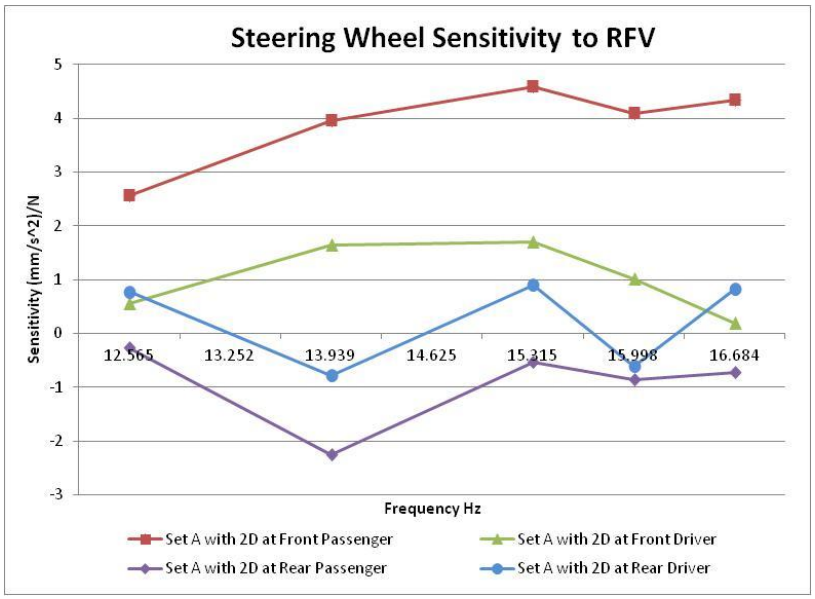

Figure 12 Steering Wheel Sensitivity to Overall Radial Force Variation

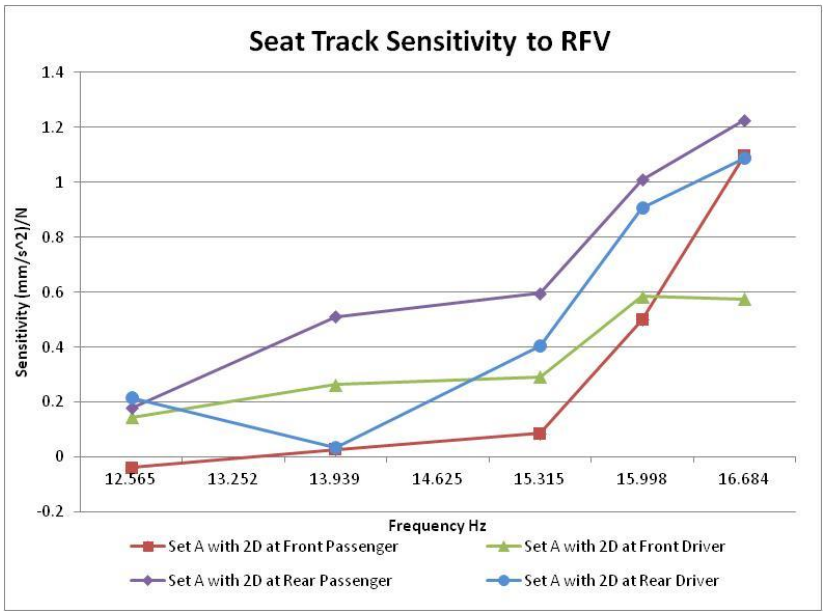

Figure 13 Seat Track Sensitivity to Overall Radial Force Variation

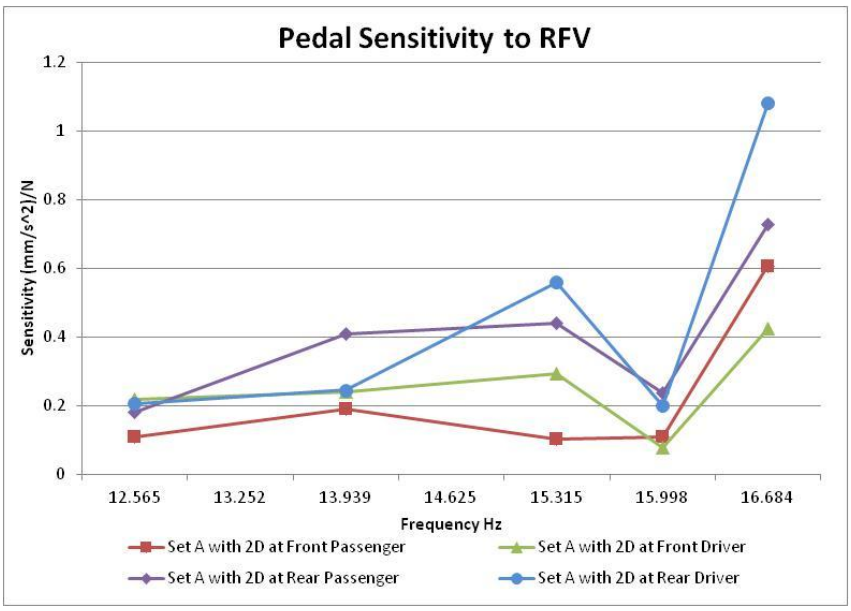

Figure 14 Pedal Sensitivity to Overall Radial Force Variation

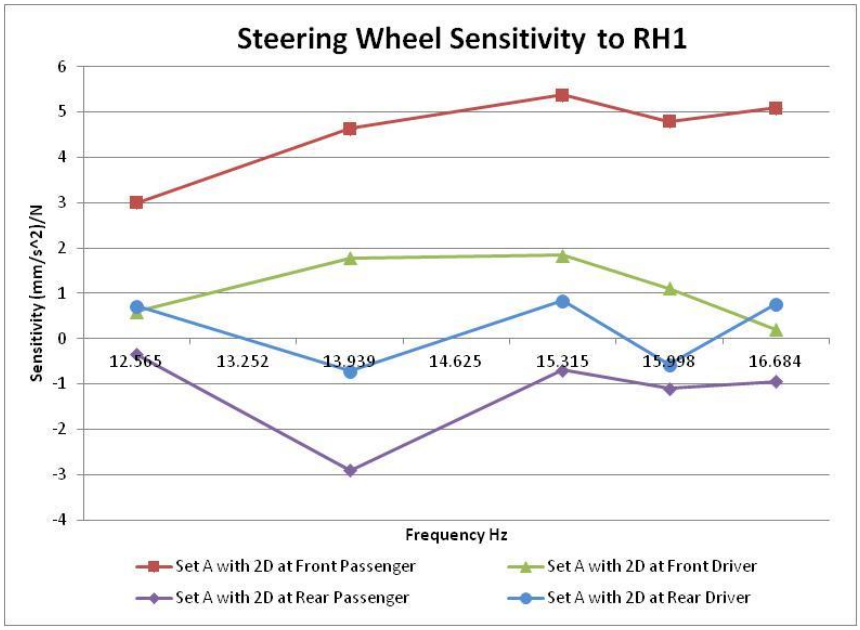

Figure 15 Steering Wheel Sensitivity to First Harmonic Radial Force Variation

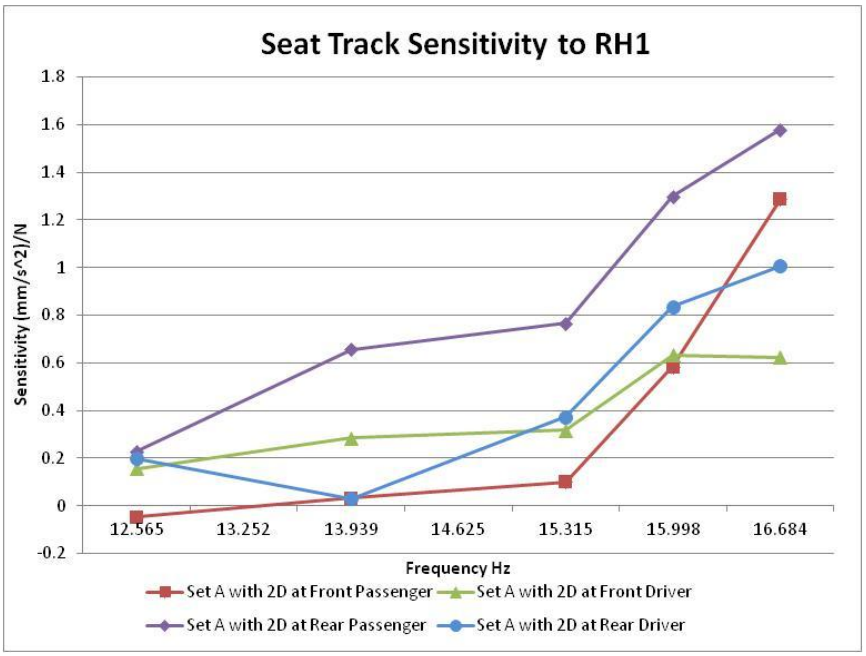

Figure 16 Seat Track Sensitivity to First Harmonic Radial Force Variation

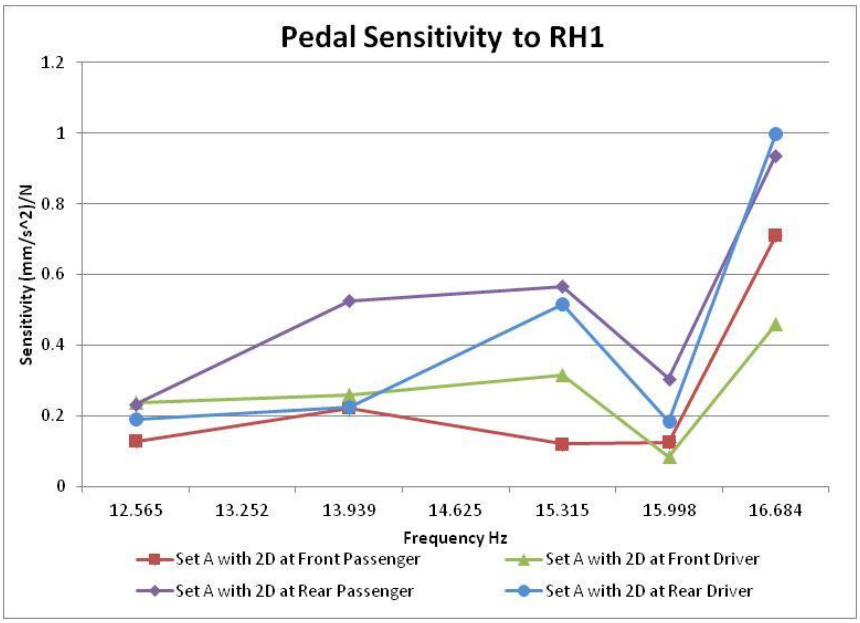

Figure 17 Pedal Sensitivity to First Harmonic Radial Force Variation

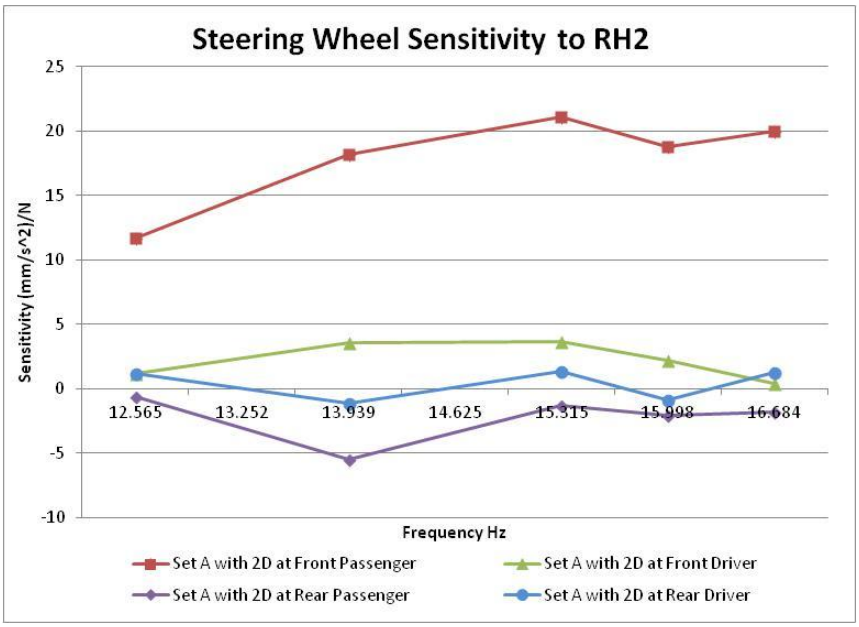

Figure 18 Steering Wheel Sensitivity to Second Harmonic Radial Force Variation

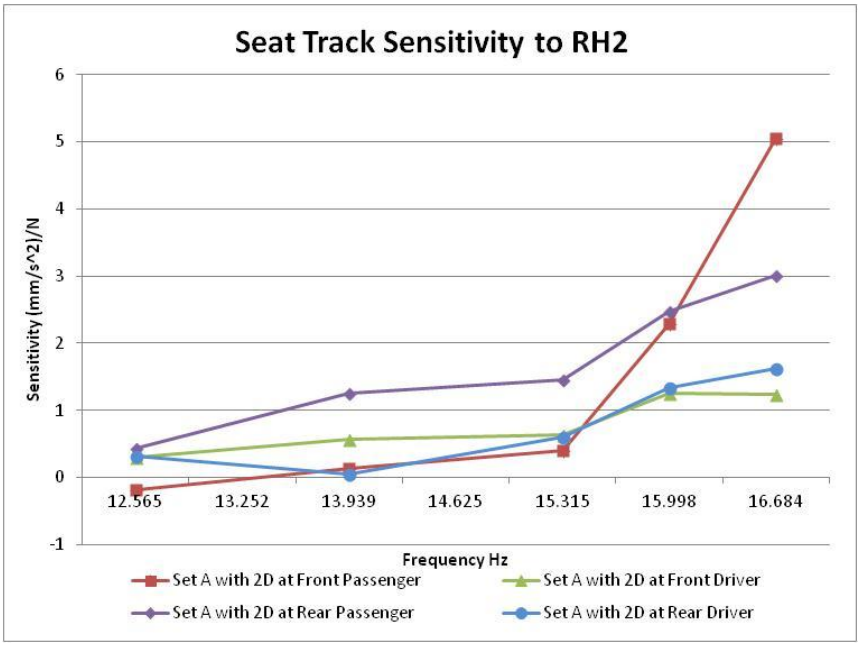

Figure 19 Seat Track Sensitivity to Second Harmonic Radial Force Variation

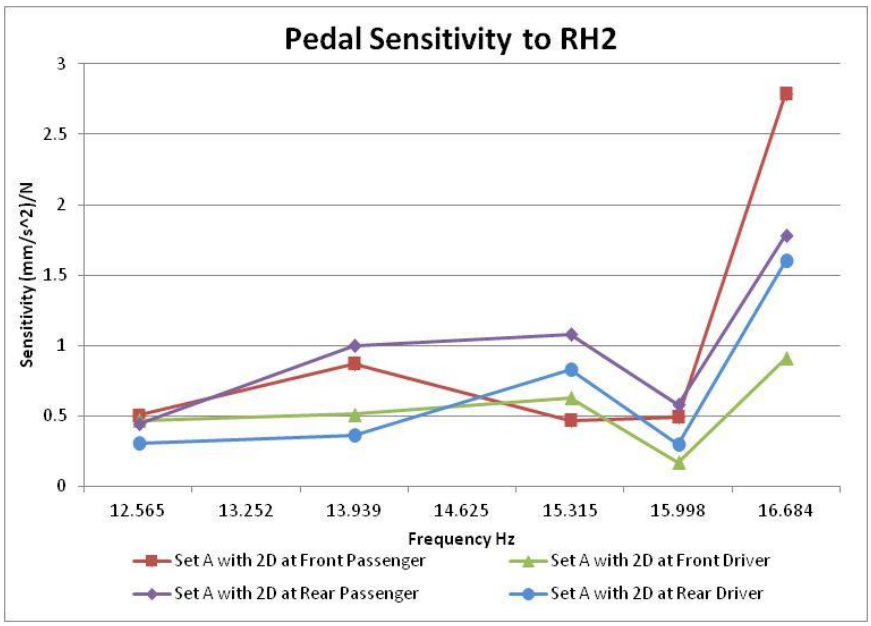

Figure 20 Pedal Sensitivity to Second Harmonic Radial Force Variation

Tangential Force Variations

Sensitivities to changes in tangential force variations at each assembly position for each CTP and test speed were evaluated using the Kokusai high-speed measurements for tangential force variation without imbalance (meaning that the non-uniformity measurements will not be affected if the assemblies are balanced later). The summary of tangential force variations for each assembly used in the testing is seen below along with the position of each Set A assembly.

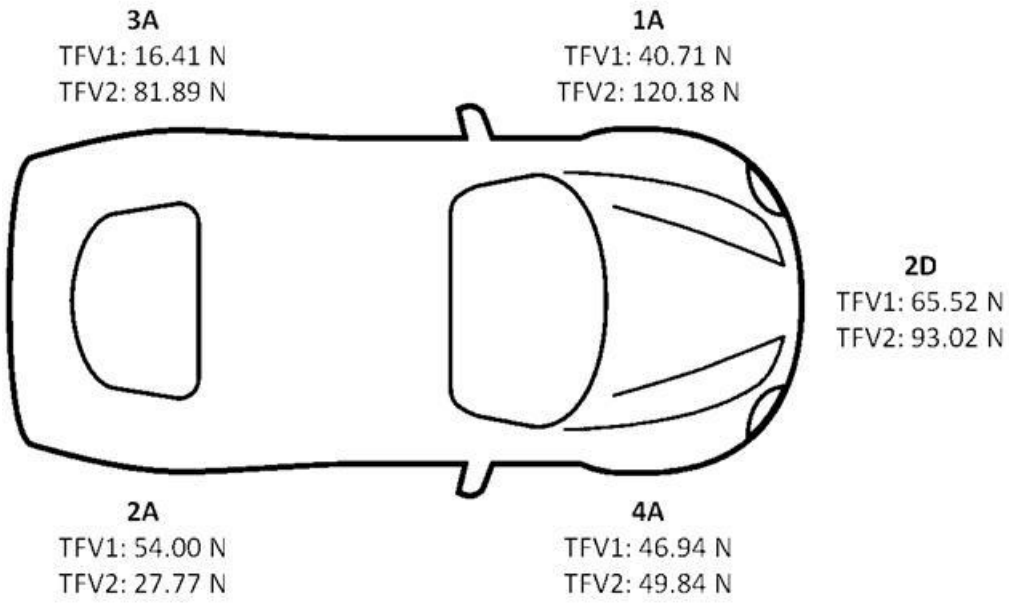

Figure 21 Tangential Force Variations and Locations of Set A and 2D Assemblies

The sensitivities to tangential force variations for each CTP and assembly position are calculated using both the maximum and average vibration recorded during the highway test runs. This produced two sensitivity curves for each force variation, CTP, and assembly position. These curves were averaged at each test speed to produce the following sensitivity curves over the frequency range relating to the first order of the test speed range of 90 to 120 kilometers per hour.

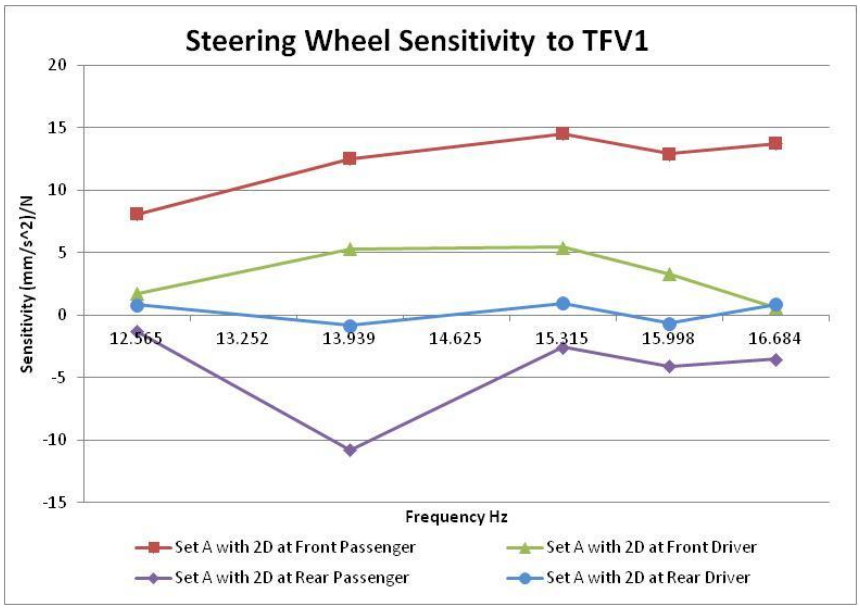

Figure 22 Steering Wheel Sensitivity to First Harmonic Tangential Force Variation

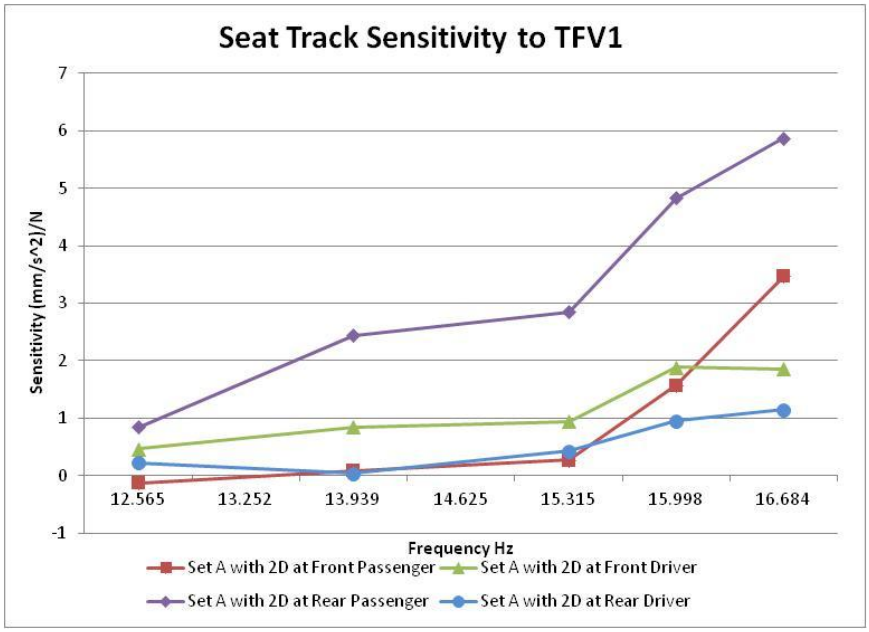

Figure 23 Seat Track Sensitivity to First Harmonic Tangential Force Variation

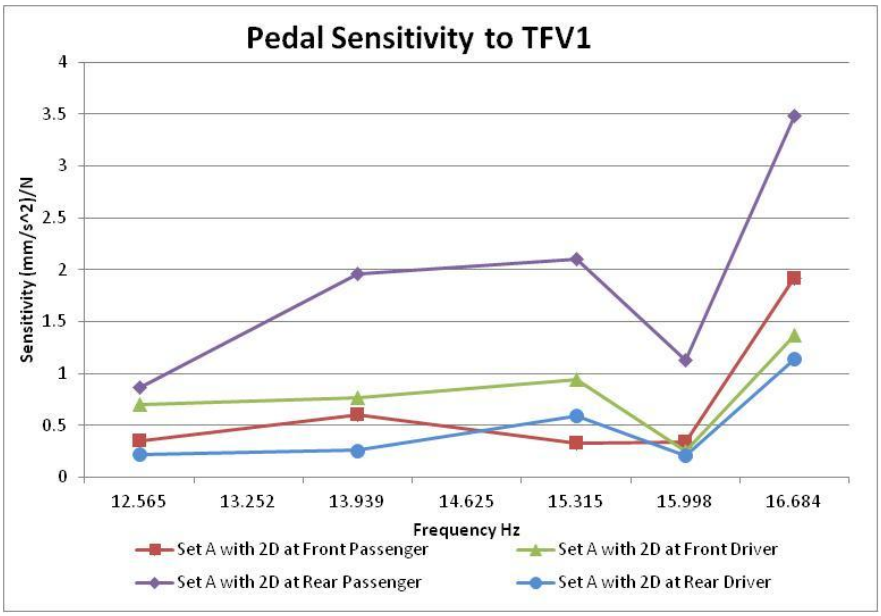

Figure 24 Pedal Sensitivity to First Harmonic Tangential Force Variation

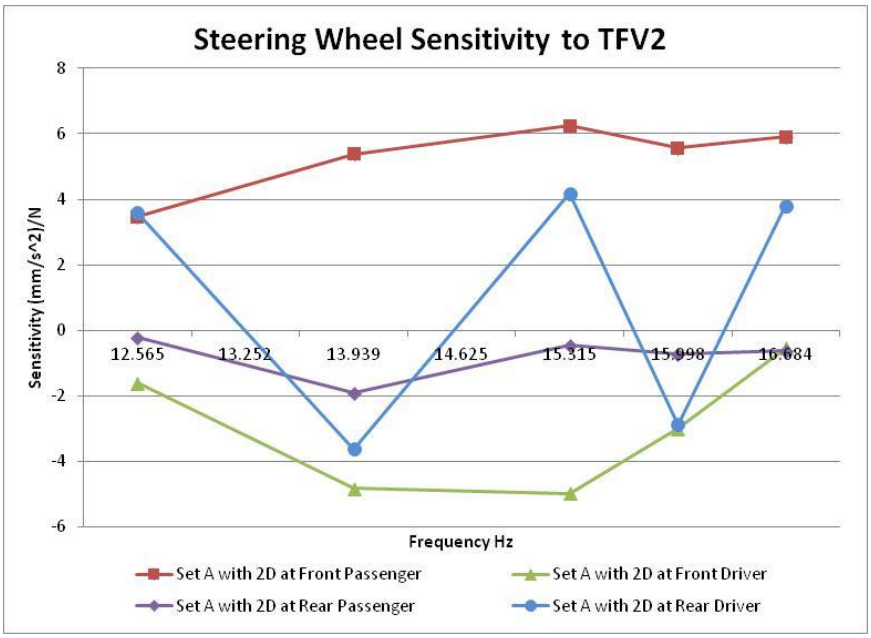

Figure 25 Steering Wheel Sensitivity to Second Harmonic Tangential Force Variation

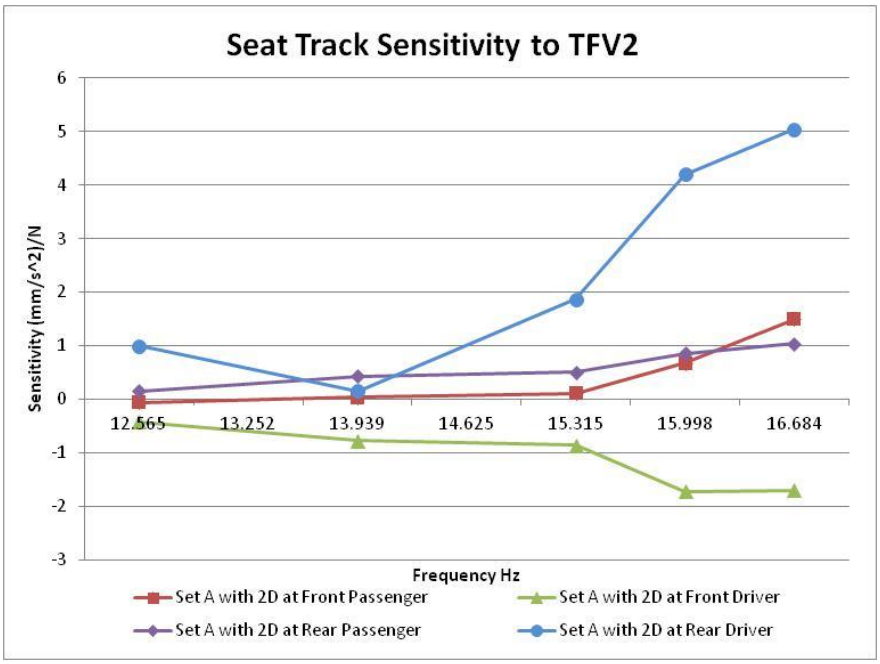

Figure 26 Seat Track Sensitivity to Second Harmonic Tangential Force Variation

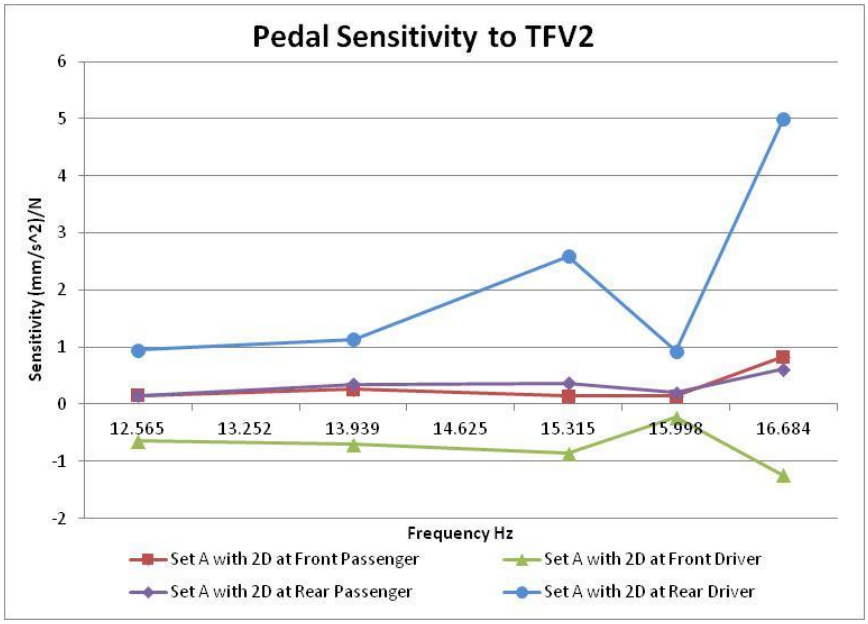

Figure 27 Pedal Sensitivity to Second Harmonic Tangential Force Variation

Radial Runout Variation

Sensitivities to changes in radial runout at each assembly position for each CTP and test speed were evaluated. The radial runount values were found using the Kokusai high speed uniformity test machine. The summary of the first harmonic radial runout for each assembly used in the testing is seen below along with the position of each Set A assembly.

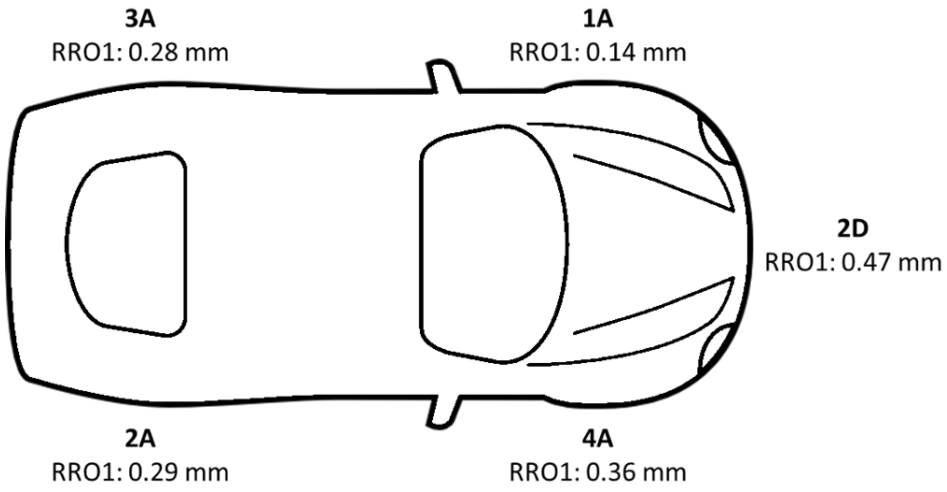

Figure 28 Radial Runout Properties and Locations of Set A and 2D Assemblies

The sensitivities to the first harmonic radial runout for each CTP and assembly position are calculated using both the maximum and average vibrations recorded during the highway test runs. This produced two sensitivity curves for each CTP and assembly position. These curves were averaged at each test speed to produce the following sensitivity curves over the frequency range relating to the first order of the test speed range of 90 to 120 kilometers per hour.

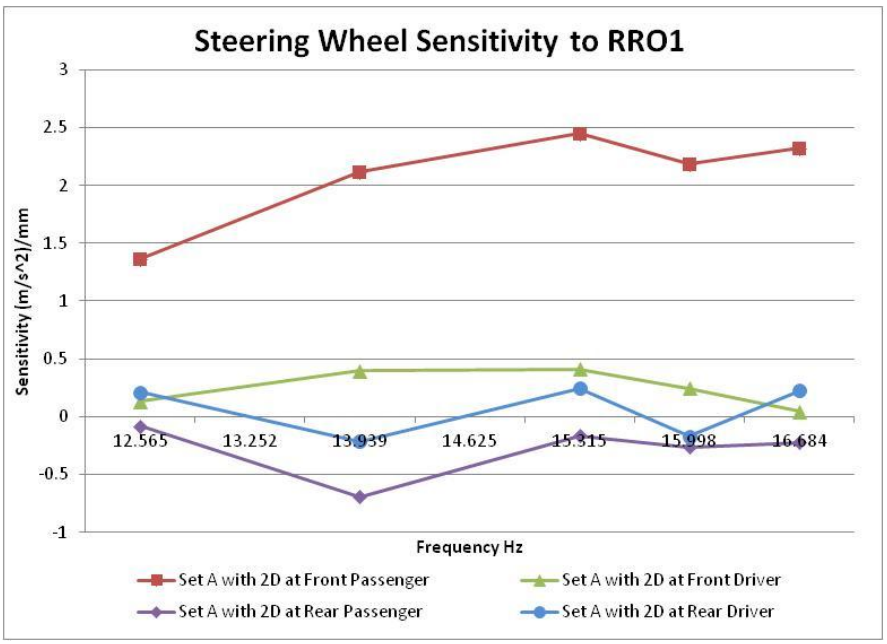

Figure 29 Steering Wheel Sensitivity to First Harmonic Radial Runout

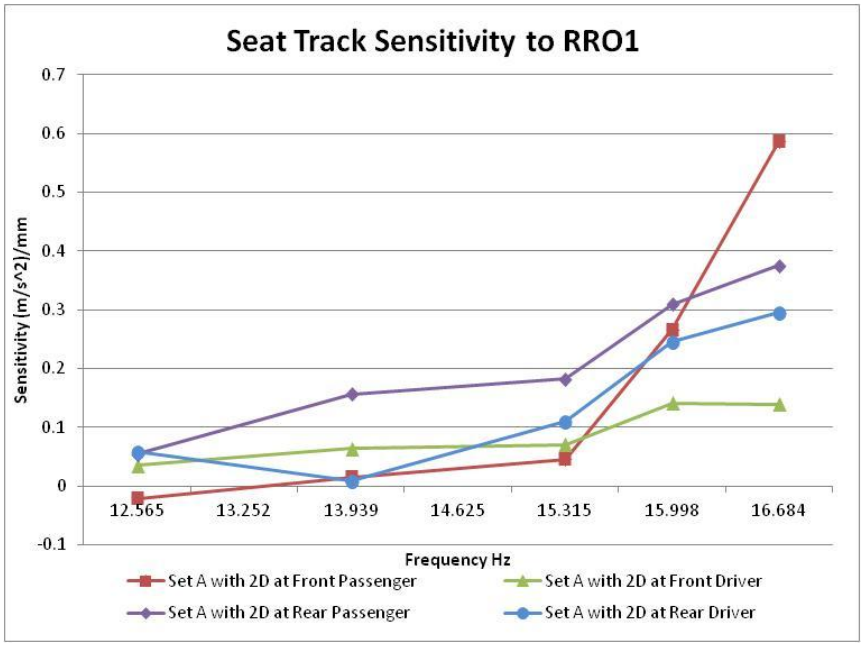

Figure 30 Seat Track Sensitivity to First Harmonic Radial Runout

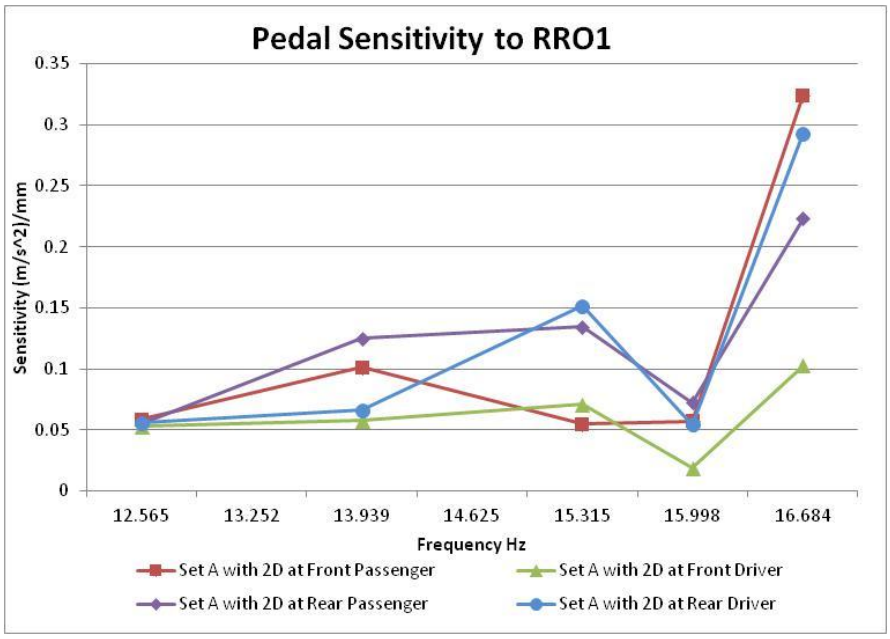

Figure 31 Pedal Sensitivity to First Harmonic Radial Runout

CHAPTER III

PREDICTING IN-VEHICLE VIBRATIONS

The goal of this research is to provide the automotive manufacturing and design engineers with a tool that will predict the in-vehicle vibrations given the batch uniformity data for tire/wheel assemblies. This tool will help the engineer assess in-vehicle NVH levels based on tire non-uniformity and, in case vibration levels do not meet the target, make the better decision of whether to request tighter control for tire uniformity or implement vehicle design changes to improve sensitivity.

Tire and Wheel Non-Uniformity Data

The automotive manufacturer provided non-uniformity data from the manufacturing plant that includes batch radial force variation, first harmonic radial force, and second harmonic radial force values for a total of 9631 tire/wheel assemblies. The automotive manufacturer also provided data from their test lab that is representative of the non-uniformity data for first harmonic radial runout, first harmonic tangential force, and second harmonic tangential force that could be expected at the manufacturing plant. The first step in the Monte Carlo process is to analyze this existing data in order to determine its statistical properties and type of distribution. After viewing the histograms of the raw data and using the identification of distribution tool in Minitab, the distributions for the non-uniformity properties were determined to have Weibull

distributions. Weibull distributions are defined with a shape and scale parameters. The scale represents the characteristic life which comprises approximately 63% of the data [6]. The following graphs show the histograms of the raw data for the non-uniformity properties compared to the Weibull distribution that best fits that data. The probability plots show how good of a fit the data is to a Weibull distribution. In the case of the radial force variations, the population size (N) is much larger than for the radial runout and tangential force variation data. Therefore, the Weibull distributions are a better fit for the radial force variation data. A larger population size for the tangential force variation and radial runout information would have improved this statistical analysis and a better fit would have been determined.

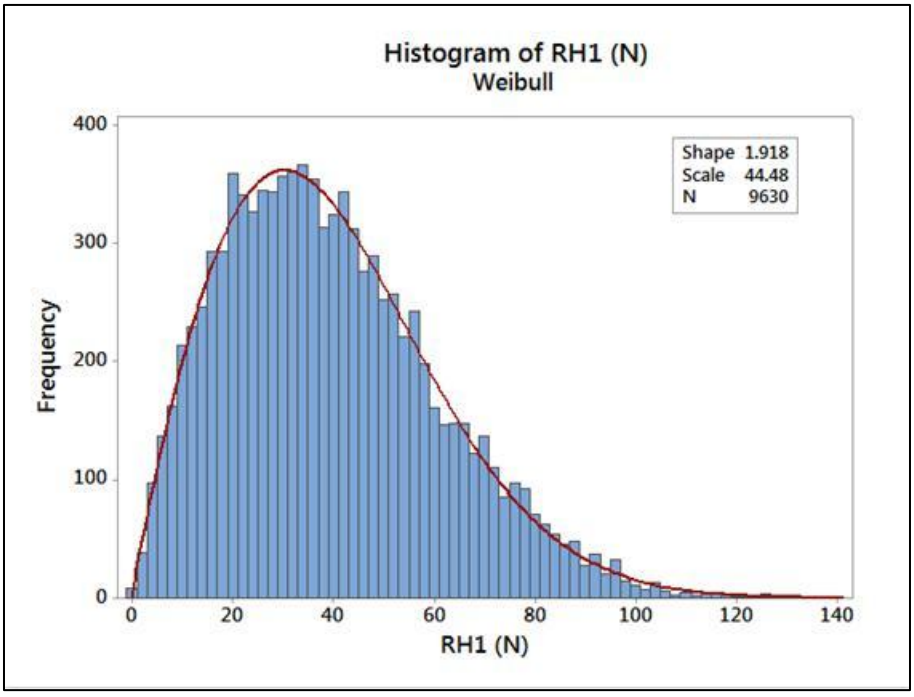

Figure 32 Histogram and Weibull distribution for first harmonic radial force variation

The histogram follows the Weibull distribution very closely for the first harmonic radial force variation data. Since the sample size is over 9600, a good fit can be determined. The shape is found to be 1.918 and the scale is 44.48. This means that approximately 63% of the RH1 values will be less than 44.48 N, and 37% of the RH1 values will be greater than 44.48 N. For a design engineer that may use this tool in the design and manufacturing phases of vehicle development, the shape and scale parameters for this non-uniformity can be modified in order to produce vehicles with acceptable vibration signatures at the CTPs. Analyzing the statistical distribution of the non-uniformities may be more advantageous than examining the specification limit for the non-uniformity alone.

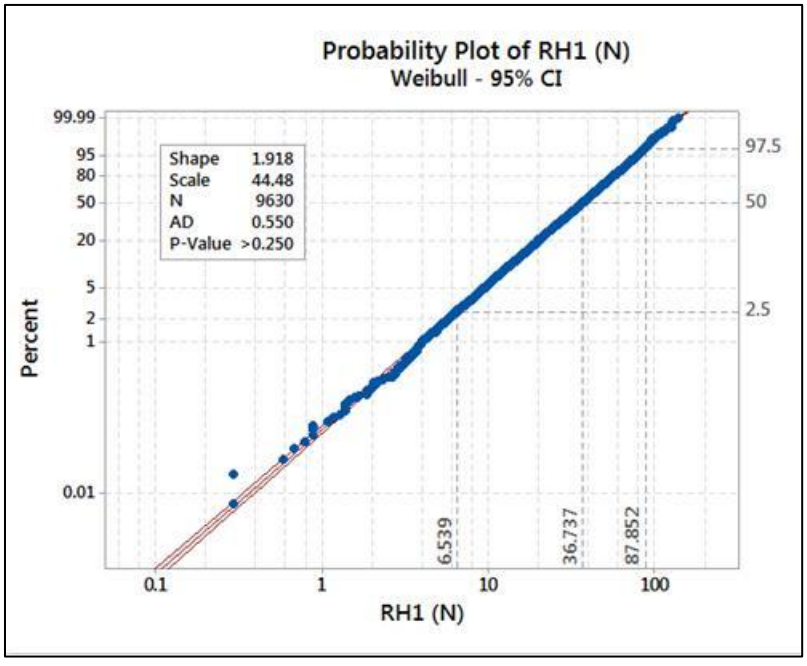

Figure 33 Probability plot for first harmonic radial force variation

The probability plot represents how well the proposed Weibull distribution fits the first harmonic radial force variation data. If the distribution were a perfect fit to the data, the blue dots would form a straight line between the red lines that represent the 95% confidence interval for the proposed Weibull distribution. Since the data being analyzed is batch data from the manufacturing plant, some outliers can be expected. This plot represents a good fit. Also shown in the probability plot are the values of RH1 that correspond to 2.5%, 50%, and 97.5% of the data.

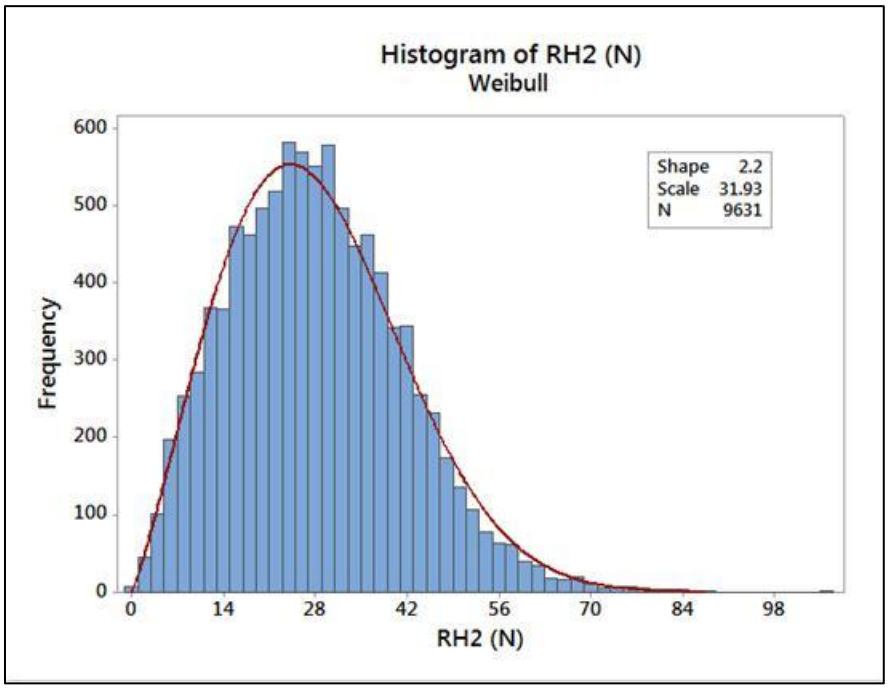

Figure 34 Histogram and Weibull distribution for second harmonic radial force variation

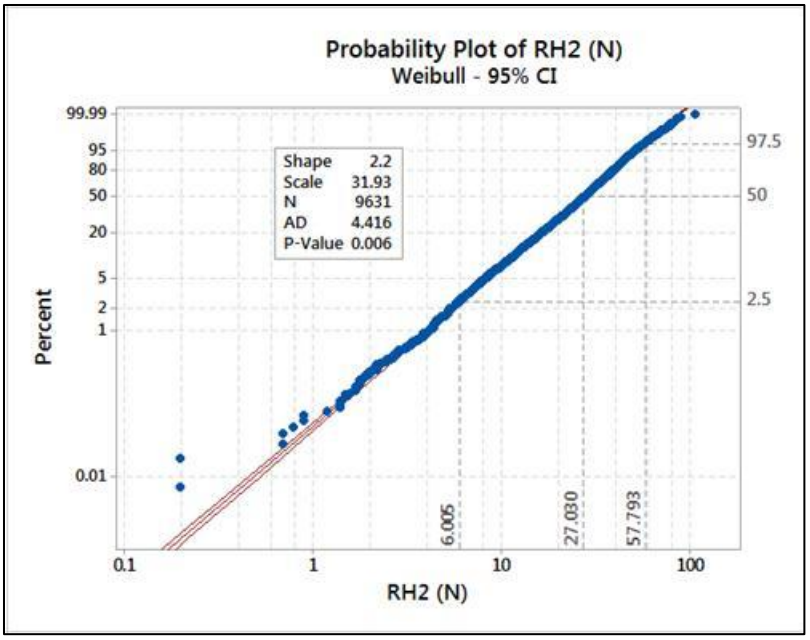

Figure 35 Probability plot for second harmonic radial force variation

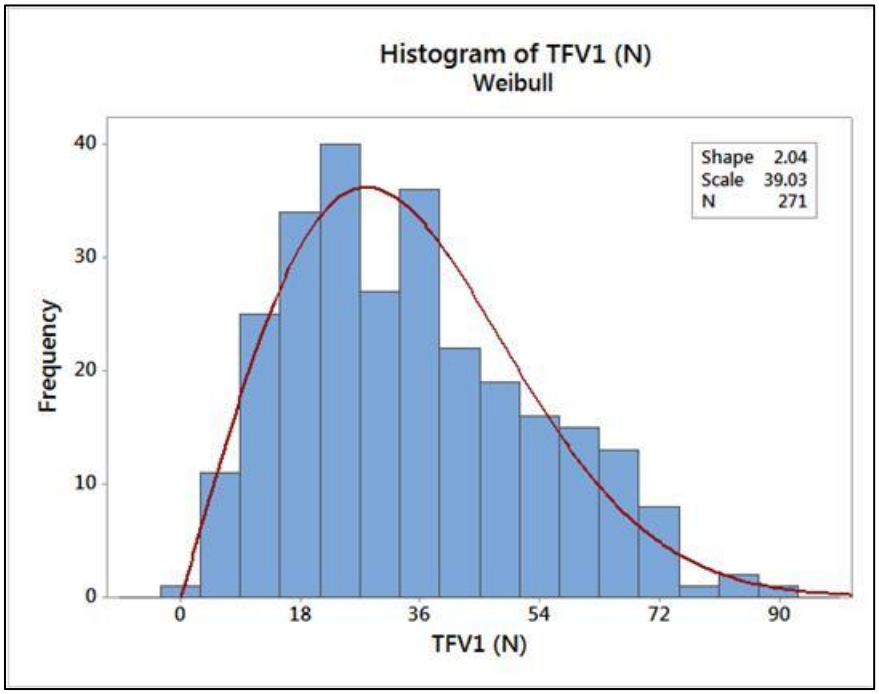

Figure 36 Histogram and Weibull distribution for first harmonic tangential force variation

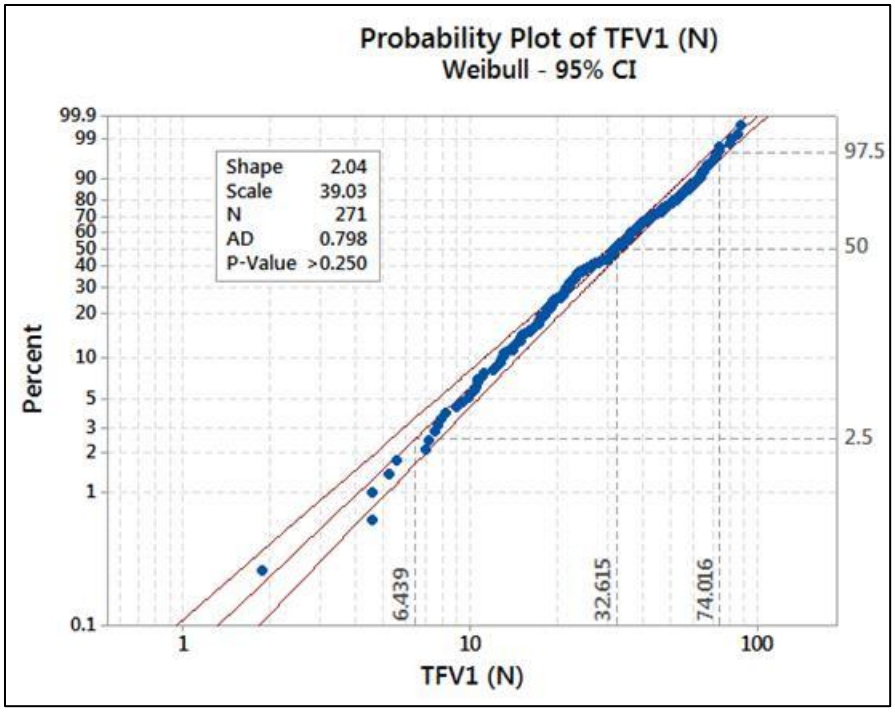

Figure 37 Probability plot for first harmonic tangential force variation

The sample size for the first harmonic tangential force variation (TFV1) data is much smaller than the radial force variation data at only 271 data points. Because of this, the histogram and Weibull distribution data are not as clearly matched as with the radial force variation data. A larger data set would allow for a more accurate statistical analysis of the data and, therefore, a better fit. However, the probability plot for TFV1 shows that the majority of the data still fits within the 95% confidence interval for the selected Weibull distribution.

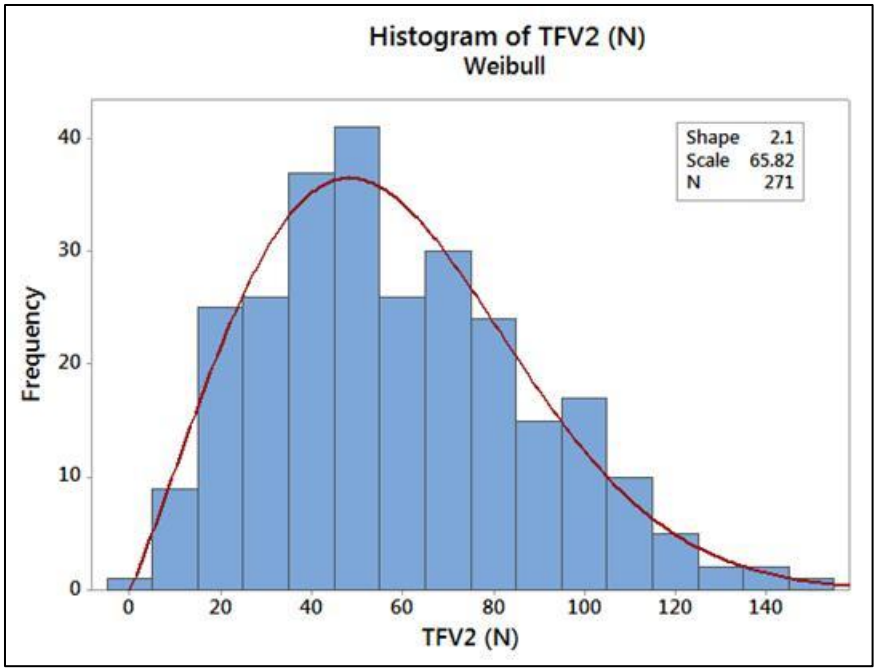

Figure 38 Histogram and Weibull distribution for second harmonic tangential force variation

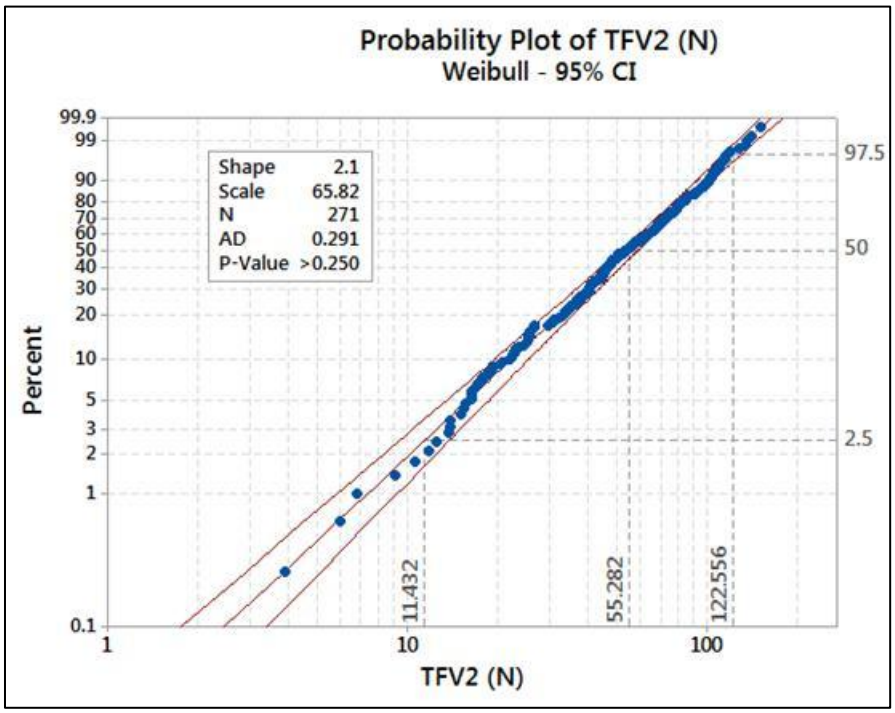

Figure 39 Probability plot for second harmonic tangential force variation

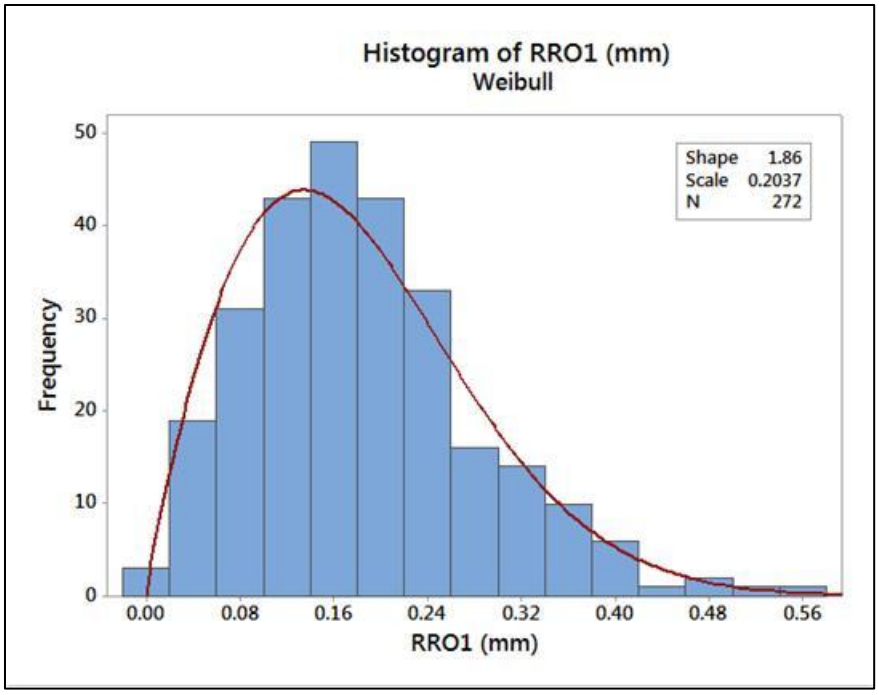

Figure 40 Histogram and Weibull distribution for first harmonic radial runout

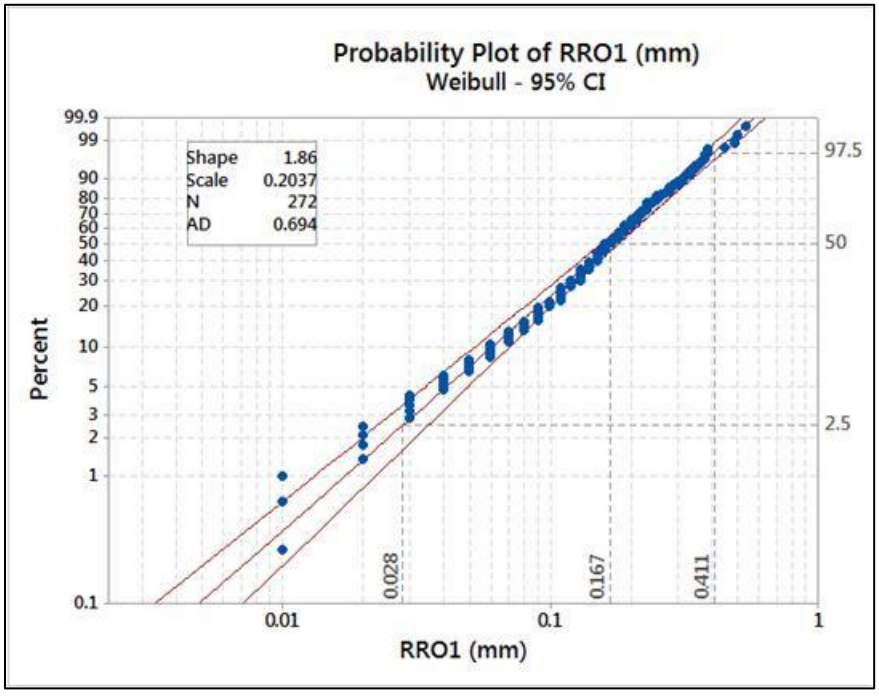

Figure 41 Probability plot for first harmonic radial runout

Unlike the distributions for the other non-uniformity properties, the overall radial force variation data relates better to a 3 parameter Weibull distribution than the previously used (2 parameter) Weibull distribution. In addition to the shape and scale properties of the distribution, there is a threshold value that signifies where the data begins. For the traditional Weibull distribution, the threshold value is 0. For the case of the overall radial force variations, the data begins at 28.06 N. This value is slightly smaller than the lowest value for overall radial force variation included in the batch data.

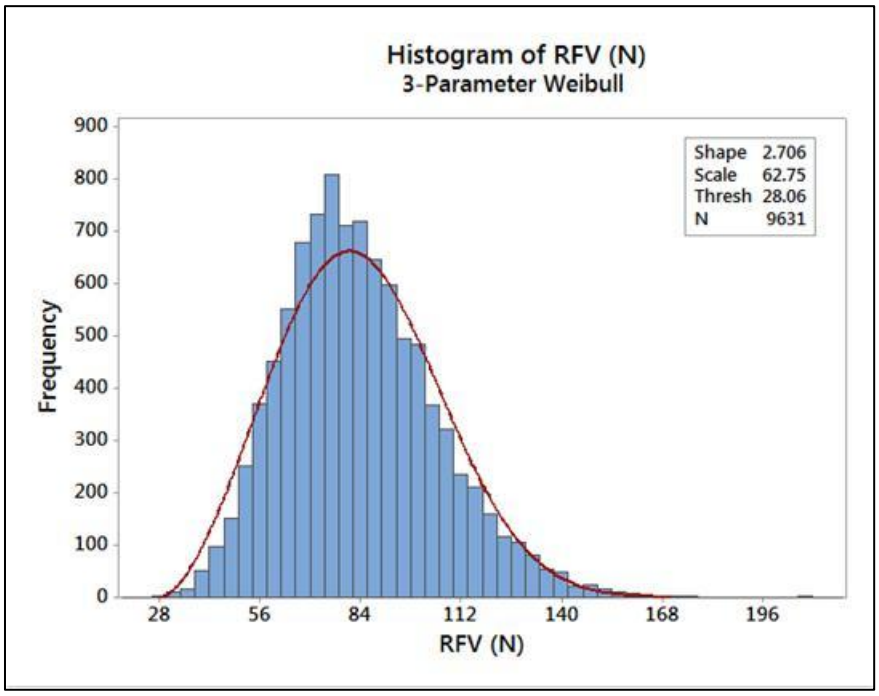

Figure 42 Histogram and Weibull distribution for overall radial force variation

Adding the threshold and scale values gives the value of the characteristic life which represents 63% of the data. In this case, 63% of the overall radial force variation data is below 90.81 N.

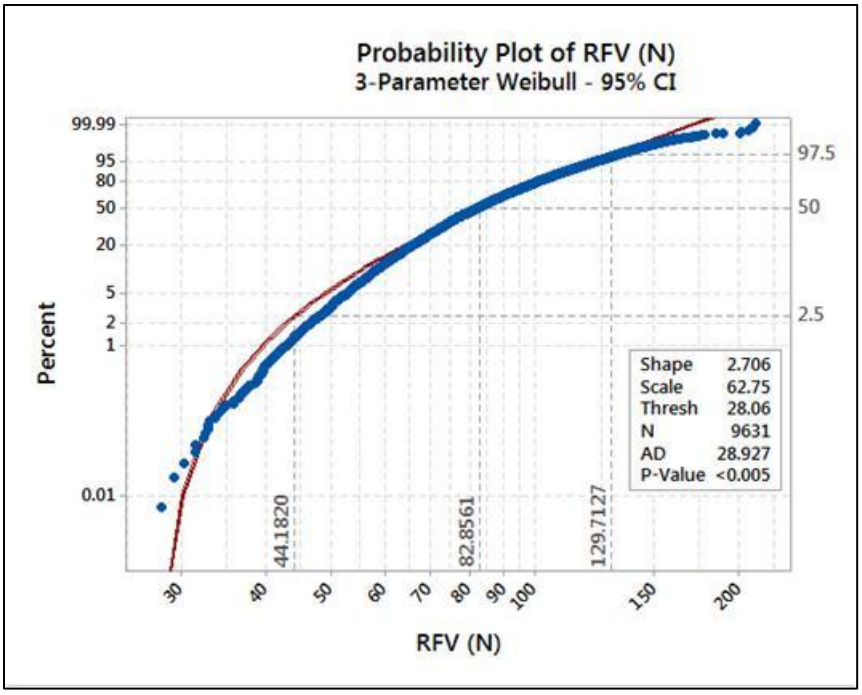

Figure 43 Probability plot for overall radial force variation

Using the shape (m) and scale (c) parameters for each force variation data set, any number of random forcing functions with the same statistical distribution as the original data can be created for the Monte Carlo analysis [7]. Equation 5 describes this calculation where x is a random number between 0 and 1 with a uniform distribution.

Eqn. 5

Equation 5 has to be altered slightly in order to calculate the overall radial force variation forcing functions due to the third parameter, threshold. The threshold value has to be added to each randomly generated forcing function.

Specification limits are defined for the first and second harmonic radial force variations and for the first harmonic tangential force variation. The limits are shown in the following chart along with the average and average plus 3 standard deviations of the Monte Carlo produced non-uniformity data for the following simulations. This graph shows that all of the simulated non-uniformity forces that have specification limits are statistically well within those limits.

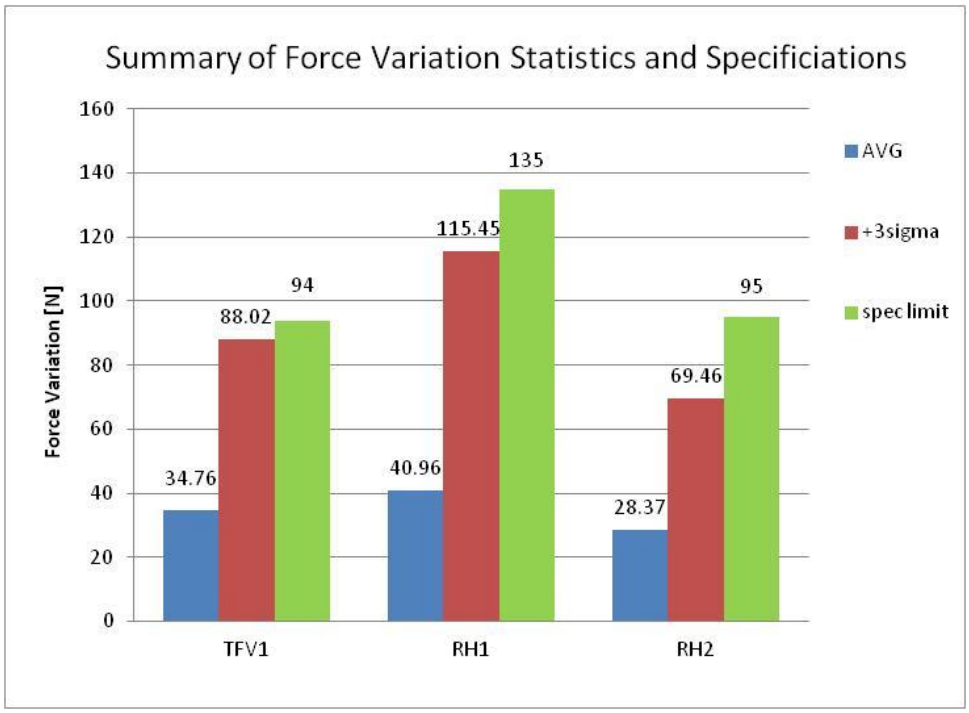

Figure 44 Specification limits and statistics for RH1, RH2, and TFV1

Predicted Vibration Results

Four Monte Carlo-generated assemblies are used to predict the total vibration felt by the customer at each CTP. For example, the first 4 random RFV values will be used for the 4 assembly positions on predicted vehicle 1. Random RFV values 5-8 are used for

vehicle 2, and so on. Starting with Equation 3 for calculating total in-vehicle response, the following equation shows how all 4 sensitivities are used to predict the total in-vehicle vibration level due to the first 4 random Monte Carlo assemblies. Unlike Equation 3, these calculations have to account for the vibration level (V_A) and forcing functions (FF_A) from the baseline setup with existing non-uniformities. The use of this equation in order to calculate the predicted in-vehicle vibration levels implies an assumption of linearity of our system (at least within the vicinity of our variations considered).

$$T \quad S \quad 1 \quad A \quad S \quad 1A \quad S_R \quad 3 \quad A$$

$$S_R \quad - \quad 3A \quad A \qquad \text{Eqn. 6}$$

Using Equation 6 and the Monte Carlo generated forcing functions, total in-vehicle vibrations can be predicted at each CTP for any number of predicted vehicle configurations. Statistical information can be determined from these results in order for the engineer to make decisions about specifications and limits for the non-uniformities of the tire/wheel assemblies or sensitivity of the vehicle.

For this research, 2400 vehicles were simulated by creating 9600 random values of non-uniformity in agreement with the statistical distribution of the assembly data at the manufacturing plant (4 values per vehicle). Expected vibration values are calculated for each CTP at each vehicle speed (i.e. frequency). The resulting predicted vibration levels represent the mean value and statistical distribution for the expected peak vibrations felt by the customer. The standard deviation is also calculated and shown with the results in

order to get an understanding of the possible range of expected vibration levels. The first standard deviation represents approximately 68% of the data. Three standard deviations represent approximately 99.97% of the data. Six standard deviations represent approximately 99.9999% of the data. If a million vibration levels were predicted, only three of those values can be expected to be greater than the value of six standard deviations. This information will be valuable for a design for six sigma approach.

Radial Force Variations

As previously discussed, the scale parameter of a Weibull distribution represents the characteristic life that is 63% of the data [6]. According to the 3 parameter Weibull distribution of the batch data for the assemblies, about 37% of assemblies can be expected to have overall radial force variation (RFV) measurements greater than 90.8 N [25]. The average value of the RFV for the batch assemblies at the plant is 83.94 N. The average value of the randomly generated RFV forcing functions is a very similar 83.91 N. This distribution will produce the predicted vibrations at the CTPs seen in the following graphs.

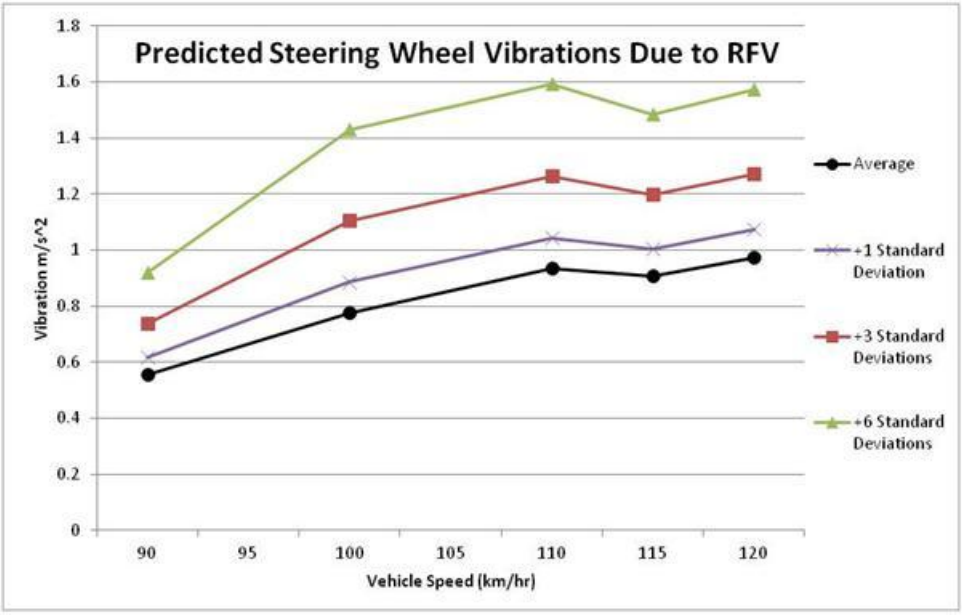

Figure 45 Predicted Steering Wheel Vibrations Due to Overall Radial Force Variations

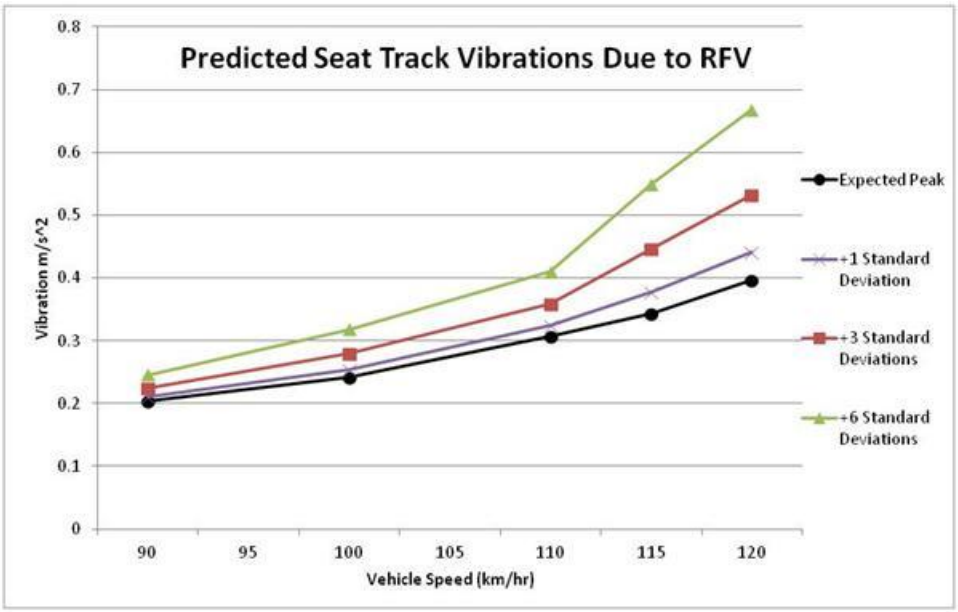

Figure 46 Predicted Seat Track Vibrations Due to Overall Radial Force Variations

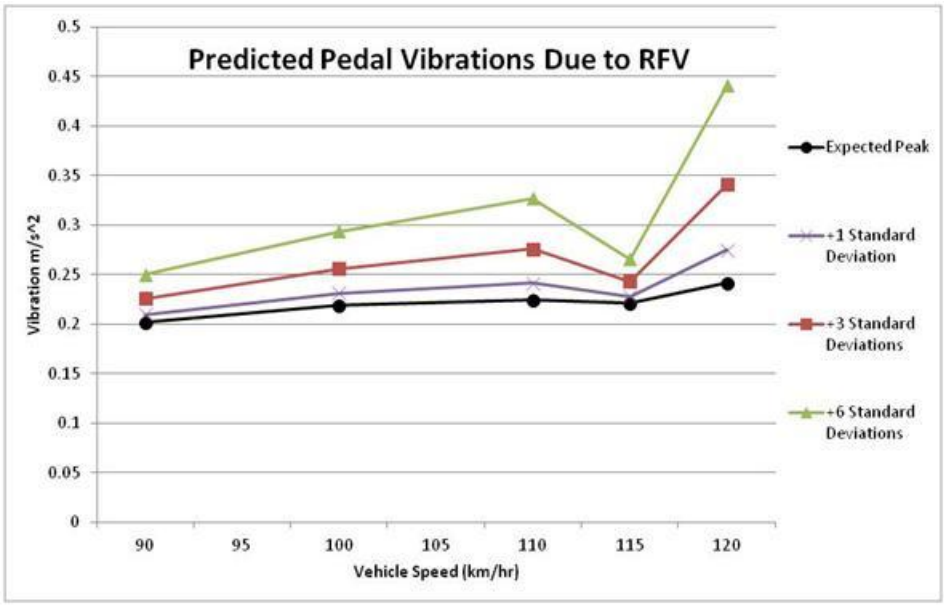

Figure 47 Predicted Pedal Vibrations Due to Overall Radial Force Variations

According to the Weibull distribution of the batch data for the assemblies, about 37% of the assemblies can be expected to have first harmonic radial force variation (RH1) measurements greater than 44.48 N [25]. The average value of the RH1 for the batch assemblies at the plant is 39.45 N. The average value of the randomly generated RH1 forcing functions is a very similar 39.27 N. This distribution will produce the predicted vibrations at the CTPs seen in the following graphs.

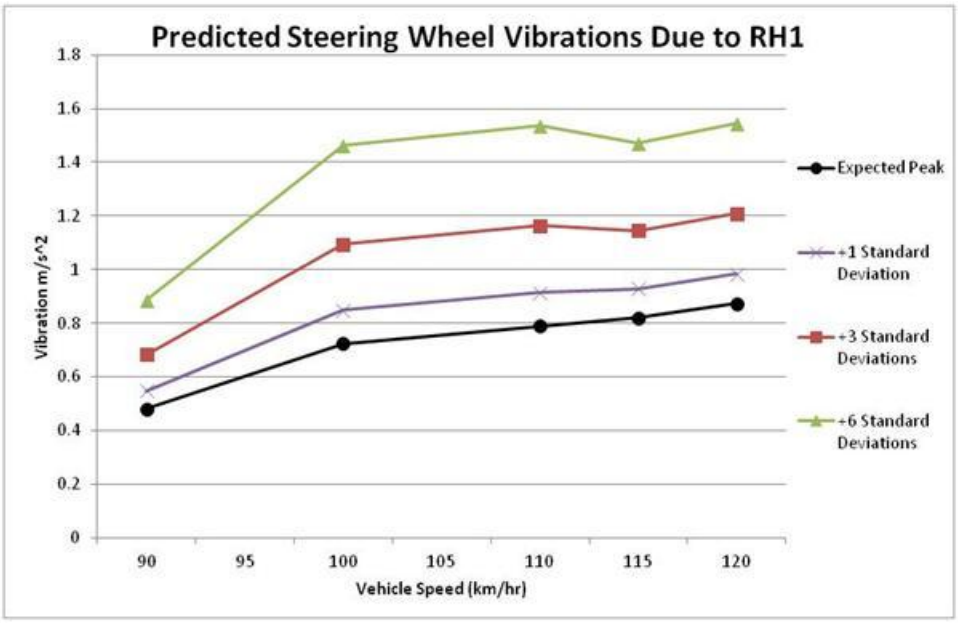

Figure 48 Predicted Steering Wheel Vibrations Due to First Harmonic Radial Force Variations

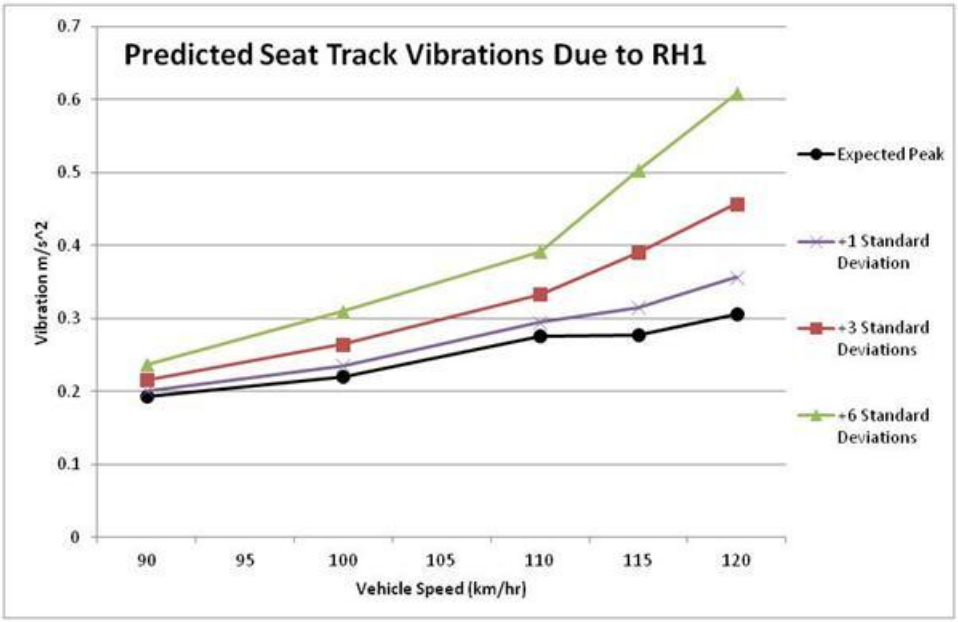

Figure 49 Predicted Seat Track Vibrations Due to First Harmonic Radial Force Variations

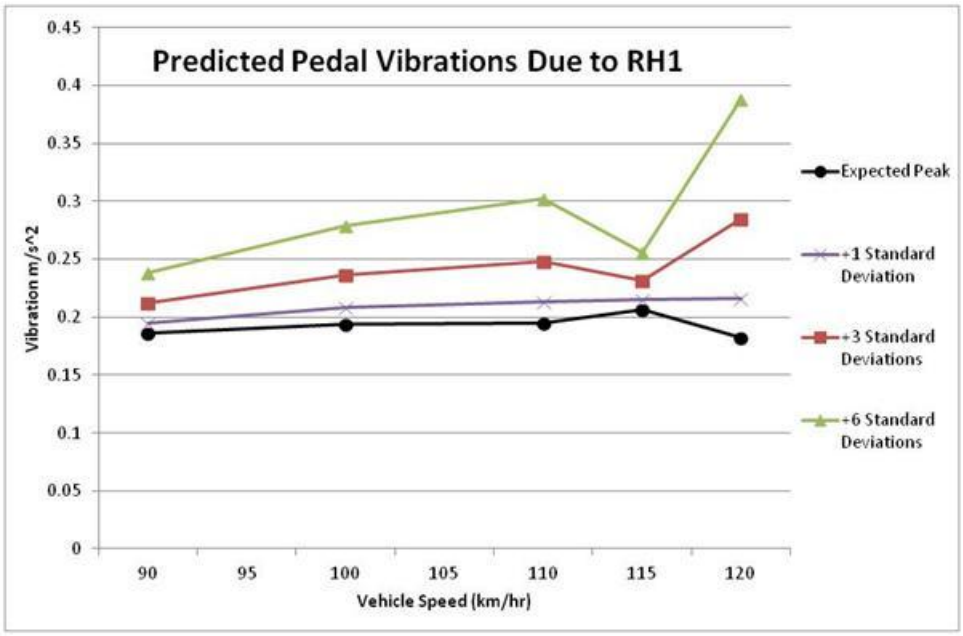

Figure 50 Predicted Pedal Vibrations Due to First Harmonic Radial Force Variations

According to the Weibull distribution of the batch data for the assemblies, about 37% of the assemblies can be expected to have second harmonic radial force variation (RH2) measurements greater than 31.93 N. The average value of the RH2 for the batch assemblies at the plant is 28.21 N. The average value of the randomly generated RH2 forcing functions is a very similar 28.37 N. This distribution will produce the predicted vibrations at the CTPs seen in the following graphs.

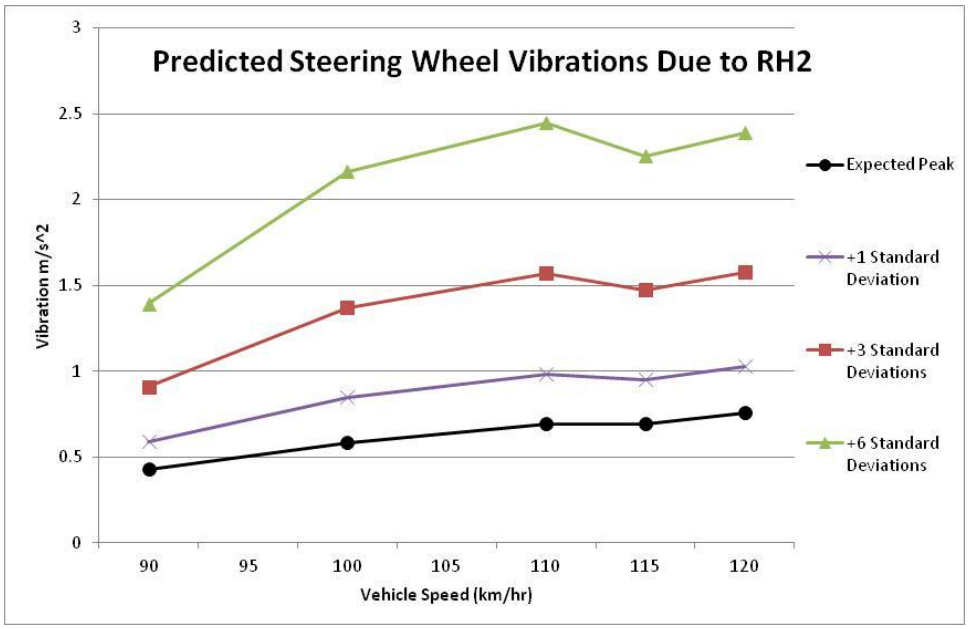

Figure 51 Predicted Steering Wheel Vibrations Due to Second Harmonic Radial Force Variation

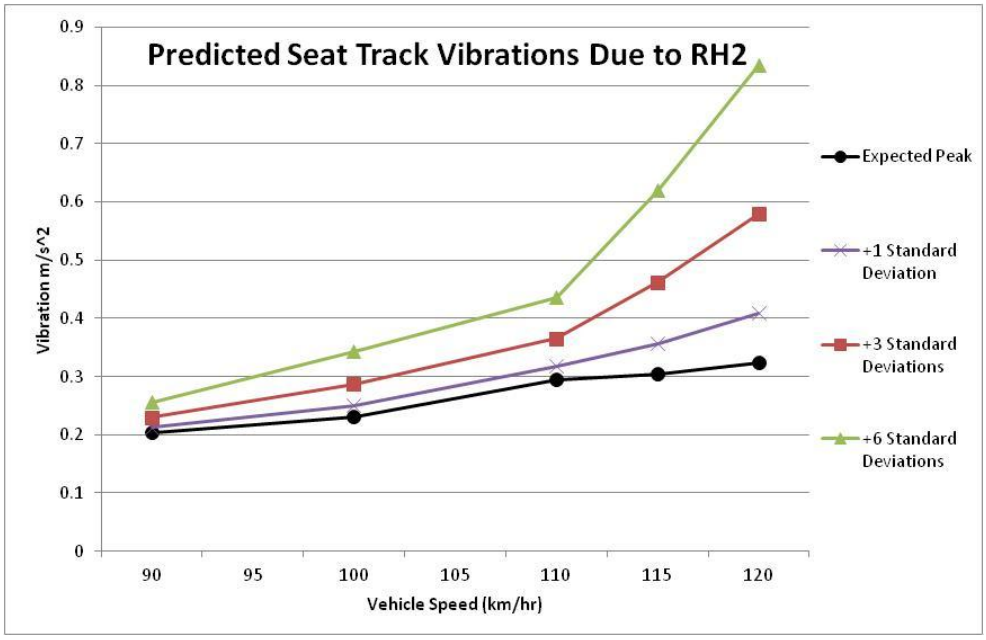

Figure 52 Predicted Seat Track Vibrations Due to Second Harmonic Radial Force Variation

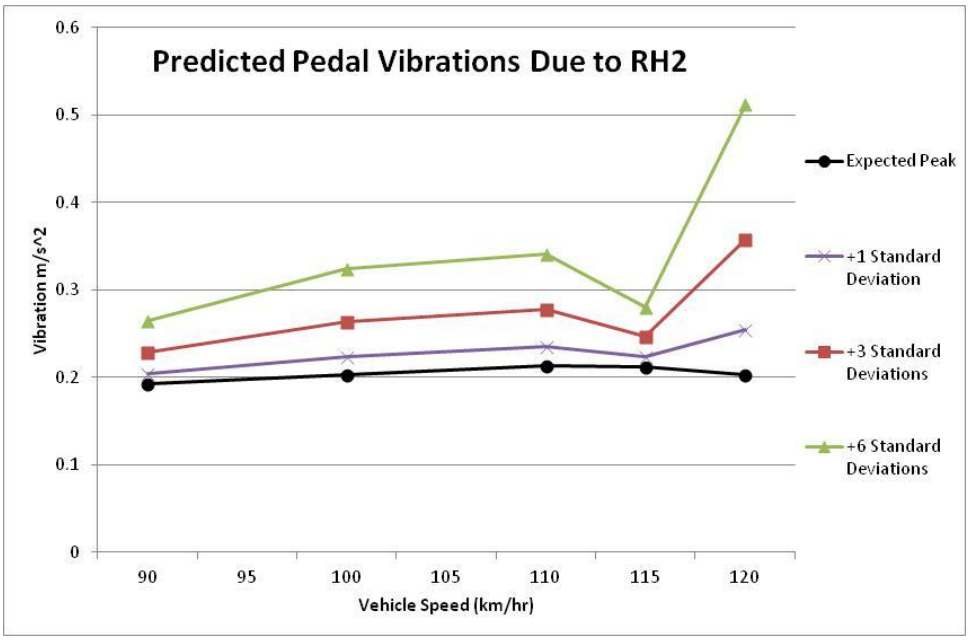

Figure 53 Predicted Pedal Vibrations Due to Second Harmonic Radial Force Variation

Tangential Force Variations

According to the Weibull distribution of the batch data for the assemblies, about 37% of assemblies can be expected to have first harmonic tangential force variation (TFV1) measurements greater than 39.03 N [25]. The average value of the TFV1 for the batch assemblies at the plant is 34.74 N. The average value of the randomly generated TFV1 forcing functions is a very similar 34.45 N. This distribution will produce the predicted vibrations at the CTPs seen in the following graphs.

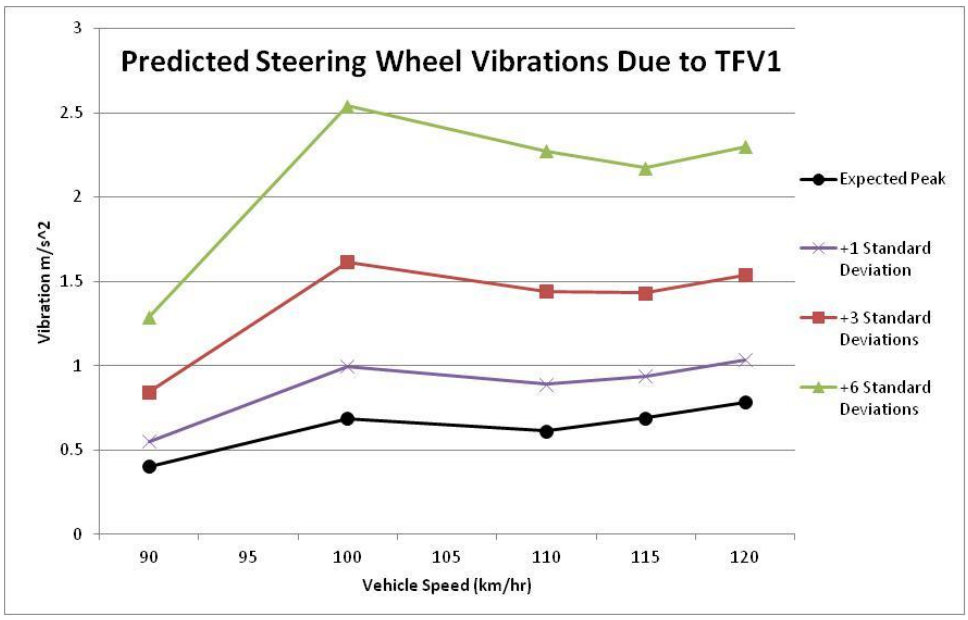

Figure 54 Predicted Steering Wheel Vibrations Due to First Harmonic Tangential Force Variations

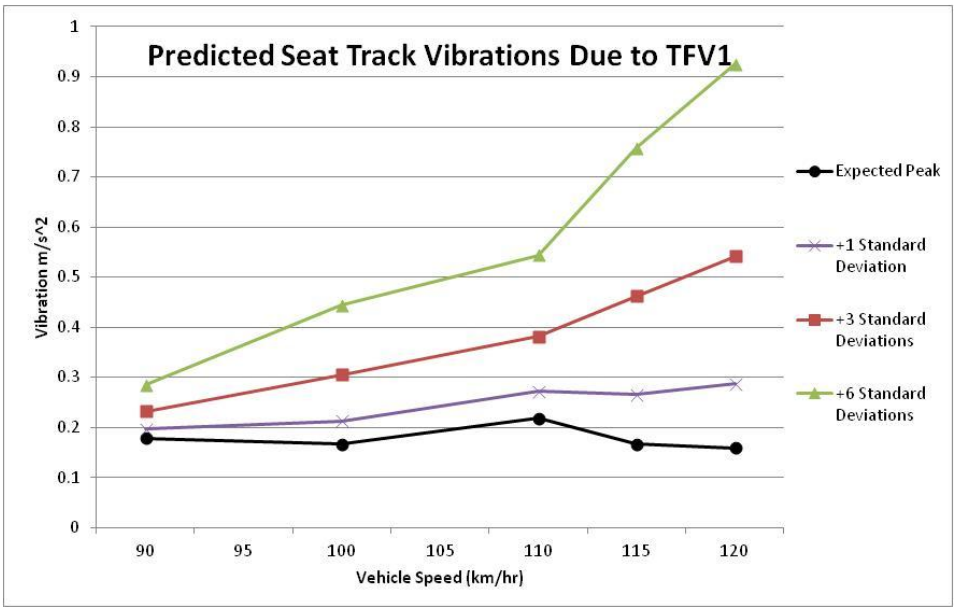

Figure 55 Predicted Seat Track Vibrations Due to First Harmonic Tangential Force Variations

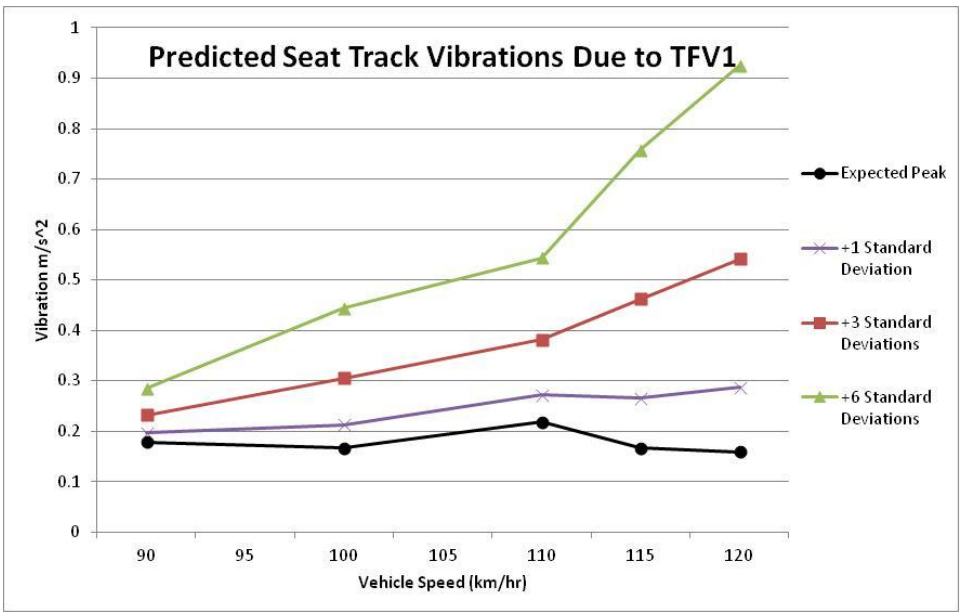

Figure 56 Predicted Pedal Vibrations Due to First Harmonic Tangential Force Variations

According to the Weibull distribution of the batch data for the assemblies, about 37% of assemblies can be expected to have second harmonic tangential force variation (TFV2) measurements greater than 65.82 N. The average value of the TFV2 for the batch assemblies at the plant is 58.38 N. The average value of the randomly generated TFV2 forcing functions is a very similar 58.86 N. This distribution will produce the predicted vibrations at the CTPs seen in the following graphs.

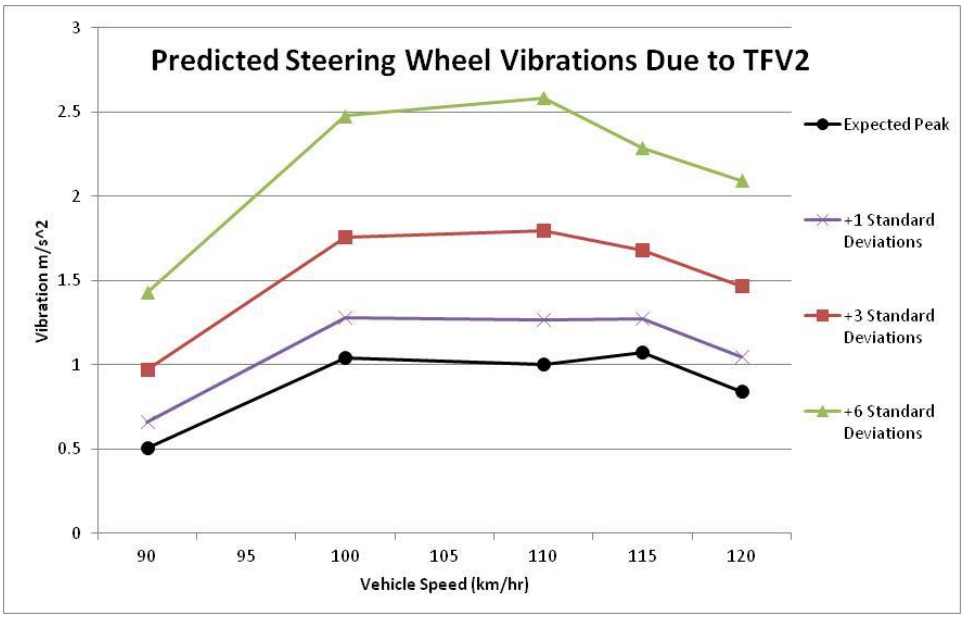

Figure 57 Predicted Steering Wheel Vibrations Due to Second Harmonic Tangential Force Variations

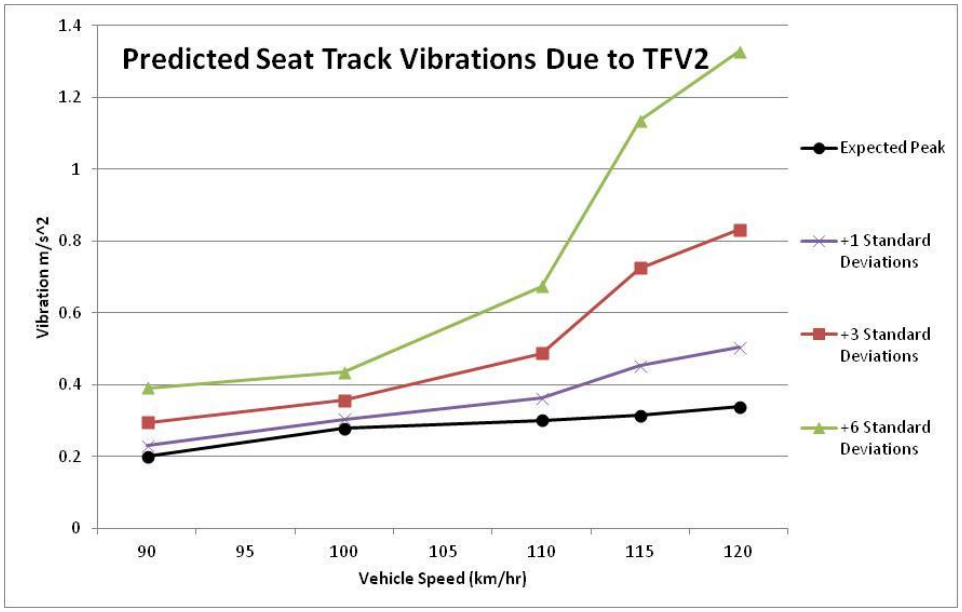

Figure 58 Predicted Seat Track Vibrations Due to Second Harmonic Tangential Force Variations

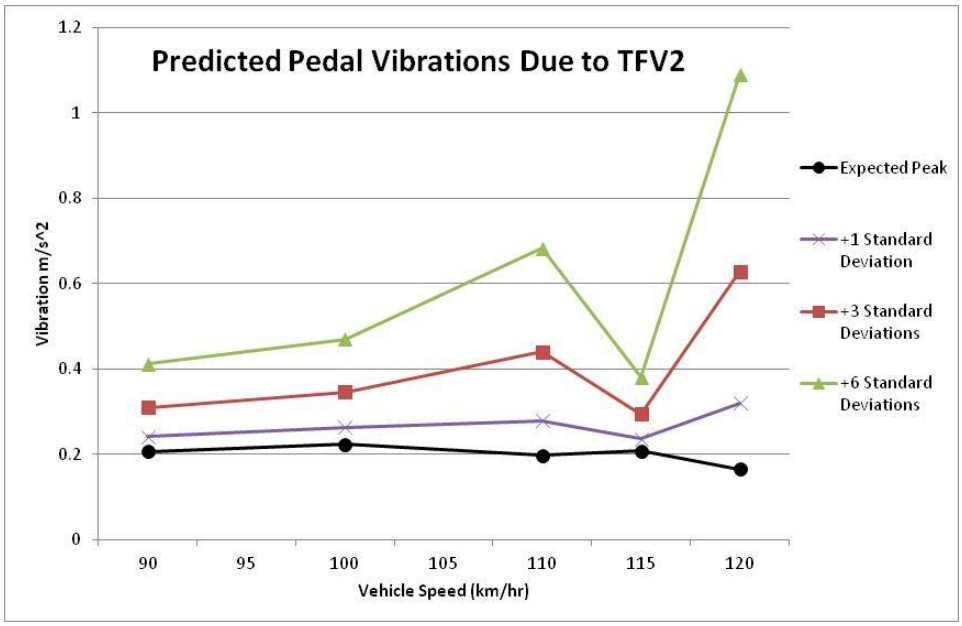

Figure 59 Predicted Pedal Vibrations Due to Second Harmonic Tangential Force Variations

Radial Runout

According to the Weibull distribution of the batch data for the assemblies, about 37% of assemblies can be expected to have first harmonic radial runout (RRO1) measurements greater than 0.2036 mm. The average value of RRO1 for the batch assemblies at the plant is 0.1795 mm. The average value of RRO1 from the randomly generated forcing functions is a very similar 0.1796 mm. This distribution will produce the predicted vibrations at the CTPs seen in the following graphs.

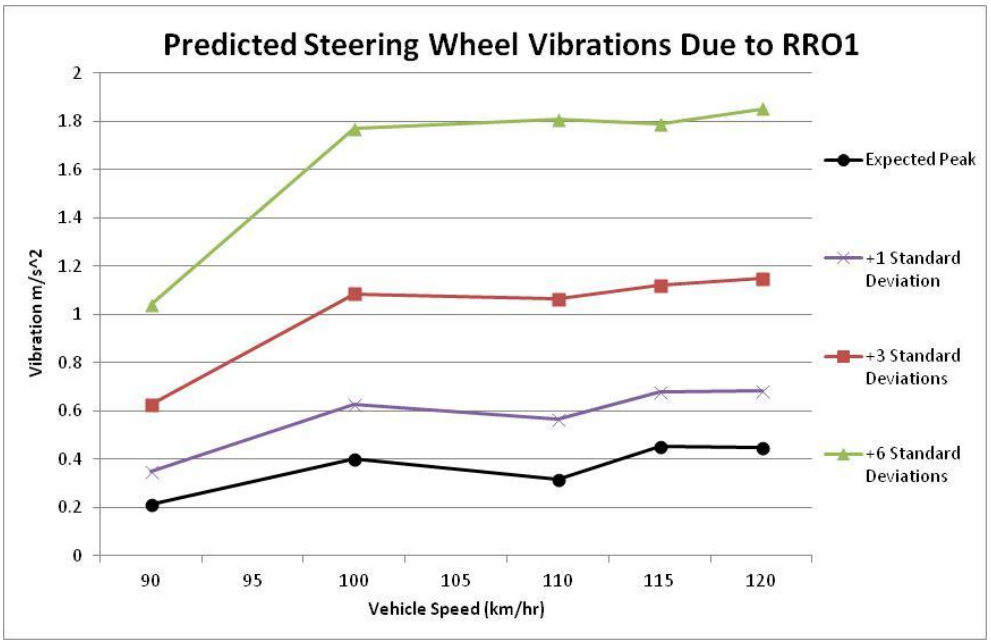

Figure 60 Predicted Steering Wheel Vibrations Due to First Harmonic Radial Runout

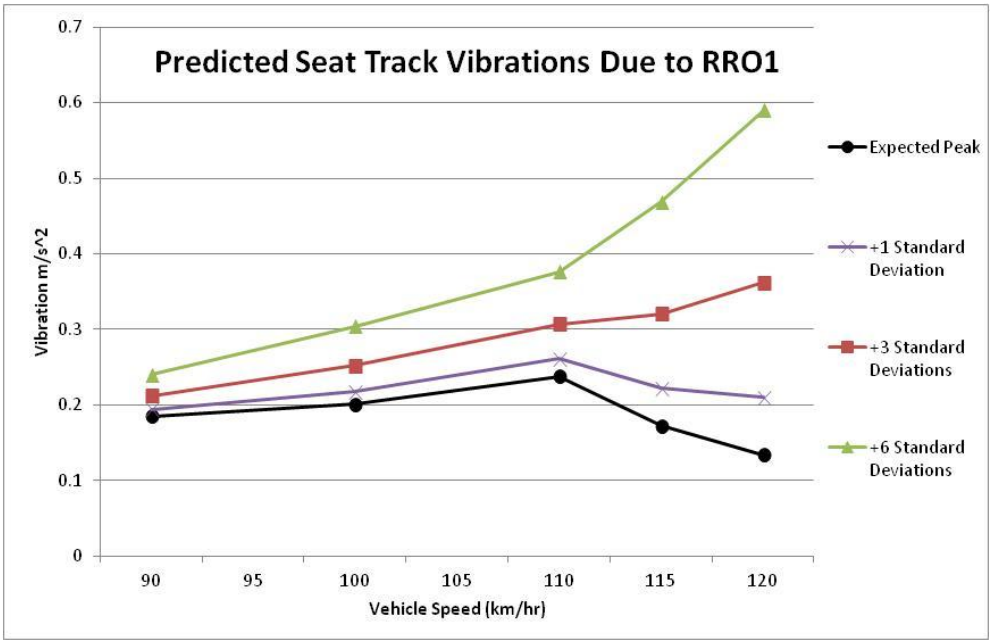

Figure 61 Predicted Seat Track Vibrations Due to First Harmonic Radial Runout

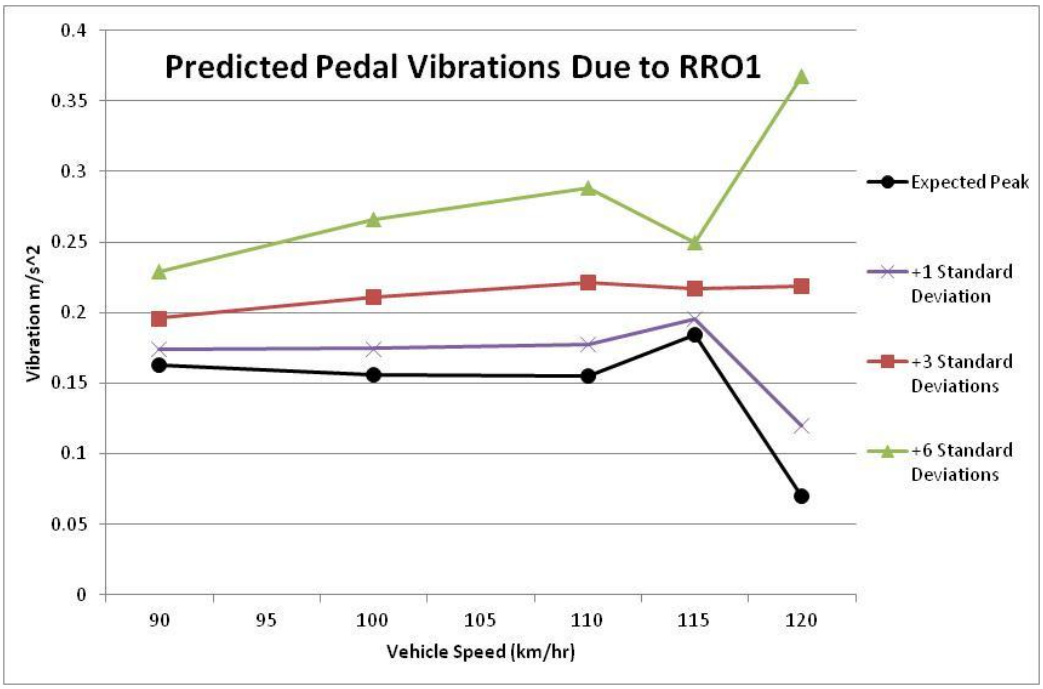

Figure 62 Predicted Pedal Vibrations Due to First Harmonic Radial Runout

CHAPTER IV

RESULTS

Looking at the predicted vibration results for each CTP can help determine which non-uniformity properties can possibly lead to excessive vibration levels that will be felt by the driver. In agreement with the warranty data for the claim of "steering wheel vibrates while driving", the highest vibration levels are seen at the steering wheel. In all cases, it is evident that the current spread of tangential force variations has the highest influence in the variation of the vibration levels felt at each CTP. The automotive engineer can now use this information to decide whether or not to improve the vehicle's sensitivity to force variations and runout of the tire/wheel assemblies or to tighten the specification limits for these non-uniformities in order to guarantee acceptable vibration levels for the driver.

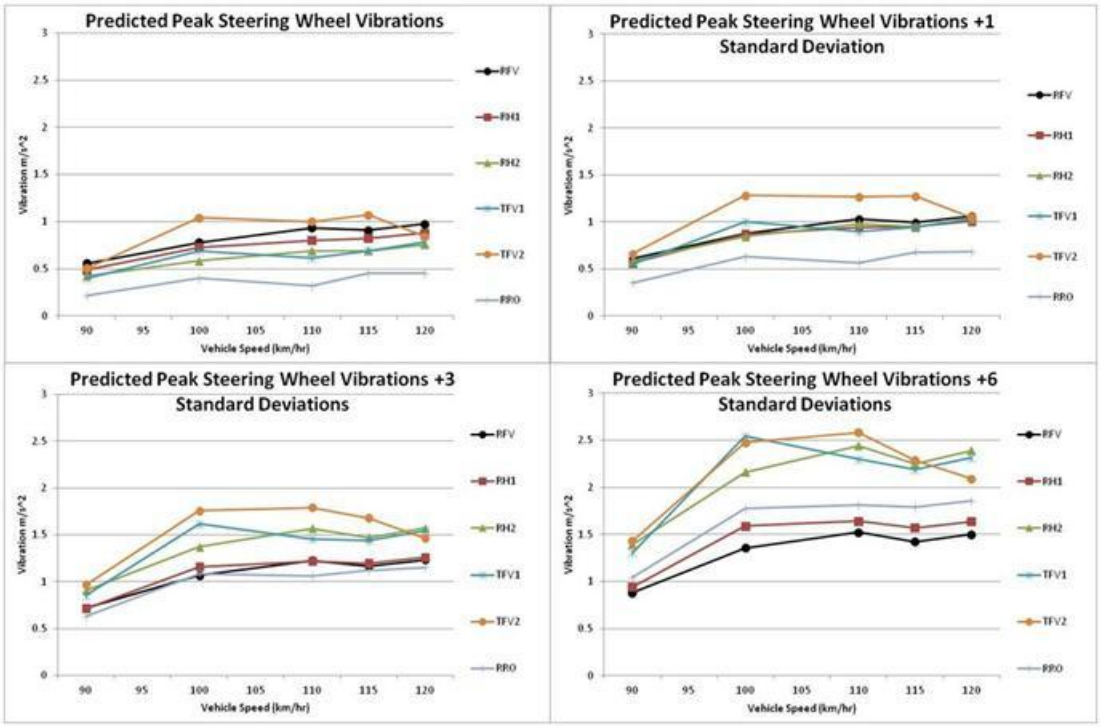

Figure 63 Comparison of Steering Wheel Vibration Levels

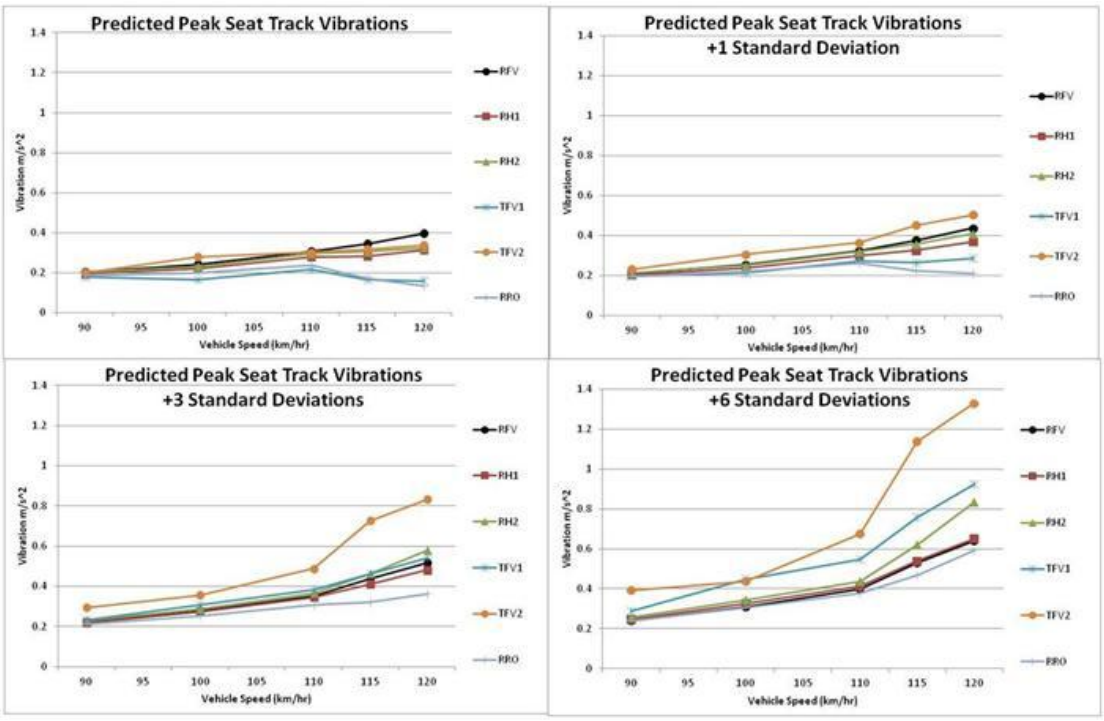

Figure 64 Comparison of Seat Track Vibration Levels

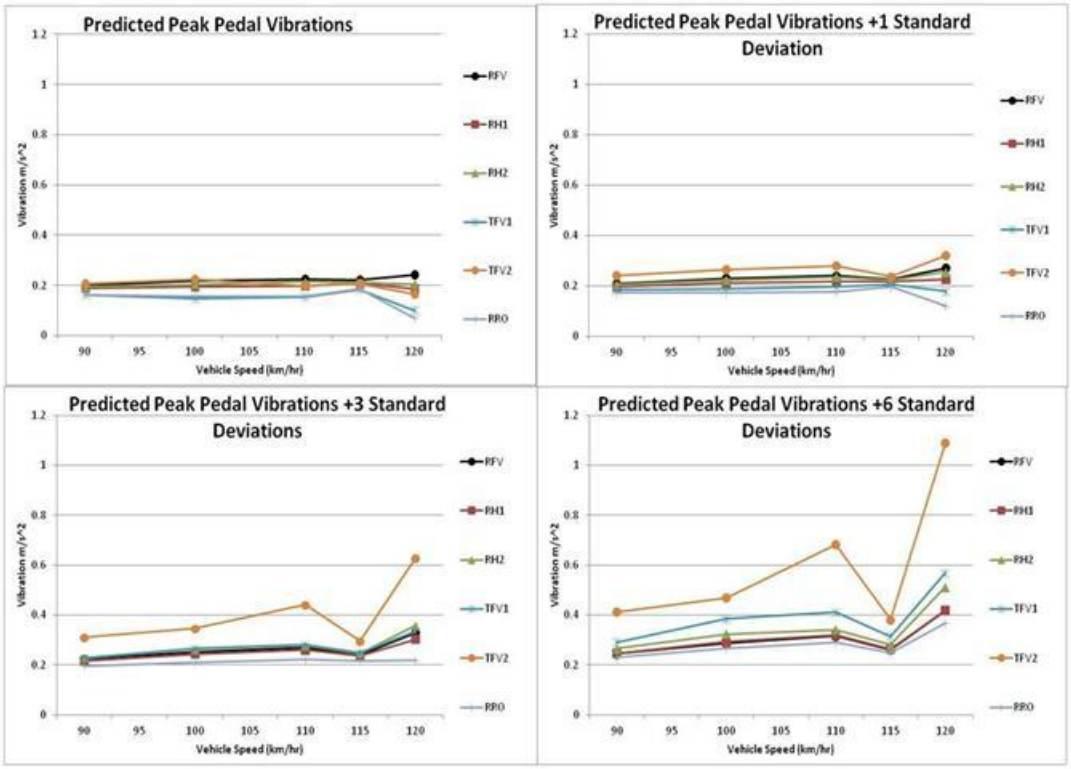

Figure 65 Comparison of Pedal Vibration Levels

The following figures compare the vibration signatures predicted during the Monte Carlo process with the test data from the in-vehicle vibration assessment. The *Set A* curve represents the peak vibrations measured during the road testing with all Set A assemblies on the vehicle. The *Maximum Seen in Testing* curve represents the maximum vibrations that were measured during any of the 5 test setups of the road testing. The points on this curve may or may not be from the same test setup. They only represent the largest vibration levels that were measured at each vehicle test speed during the in-vehicle vibration assessment. The *Monte Carlo Avg* curve is the same as the *Average* or *Expected Peak* curves on the figures with the standard deviations in the *Predicted Vibration Results* section. This curve is made up of the average vibration level that was

predicted by the Monte Carlo process for each vehicle speed. The *Monte Carlo Max* and *Monte Carlo Min* curves are made up of the maximum and minimum vibration levels that were predicted by the Monte Carlo process for each vehicle test speed. The *All 2D Assemblies* curve is a simulated vibration signature of the expected vibration levels that could be expected if assembly 2D were theoretically mounted in each of the 4 positions on the vehicle. Similarly, the *All 1A Assemblies* curve simulates the scenario where assembly 1A is mounted at each of the 4 positions on the vehicle. Assembly 2D has the highest values of radial force variations among all test assemblies, and assembly 1A has the lowest value of radial force variations among the actual assemblies used during the in-vehicle vibration assessment.

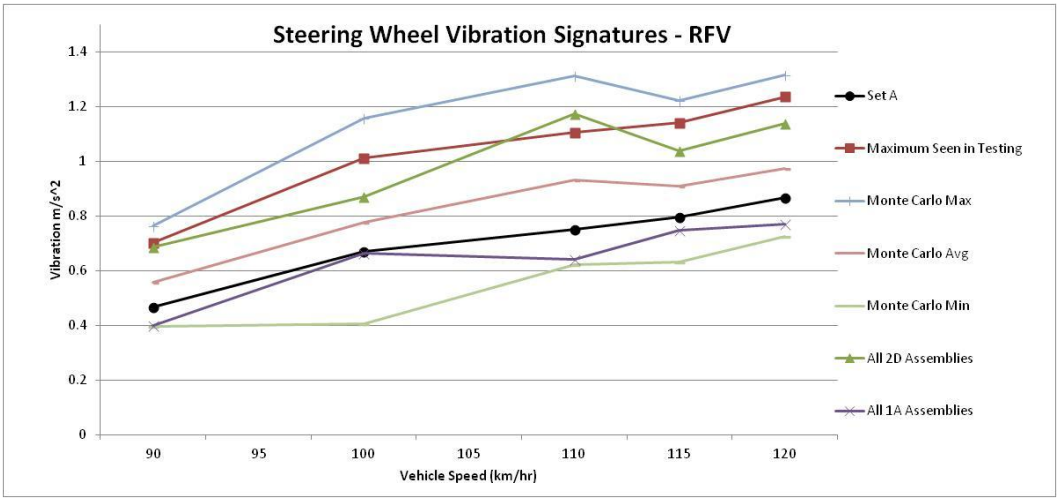

Figure 66 Comparison of Steering Wheel Vibration Signatures Due to RFV

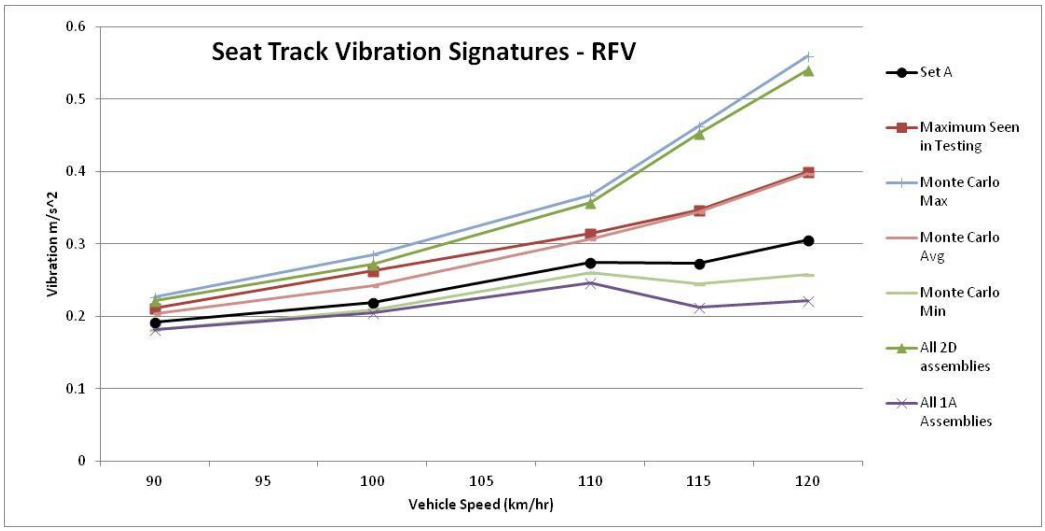

Figure 67 Comparison of Seat Track Vibration Signatures Due to RFV

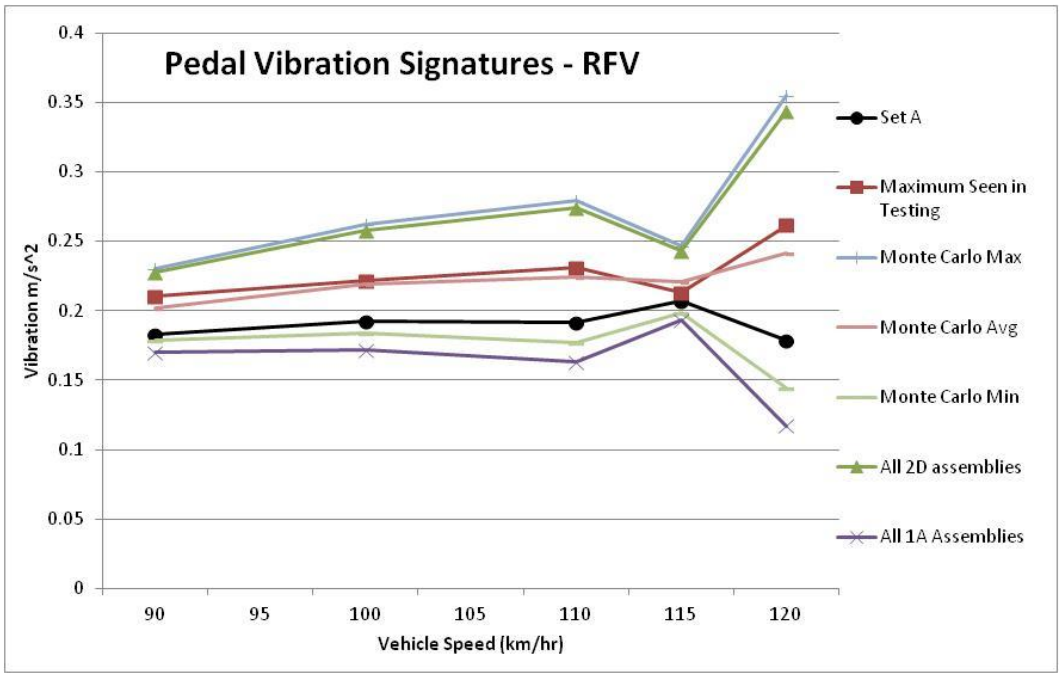

Figure 68 Comparison of Pedal Vibration Signatures Due to RFV

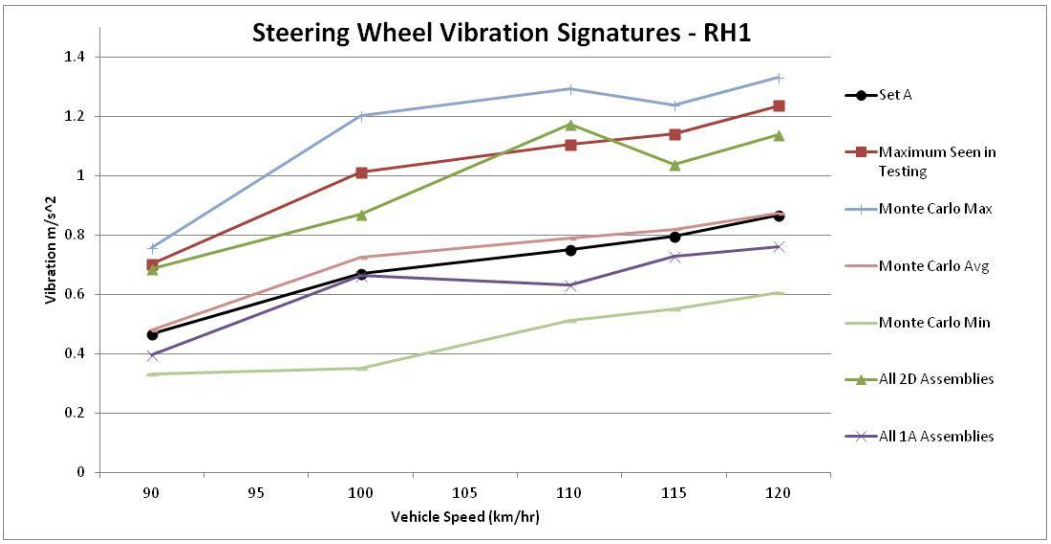

Figure 69 Comparison of Steering Wheel Vibration Signatures Due to RH1

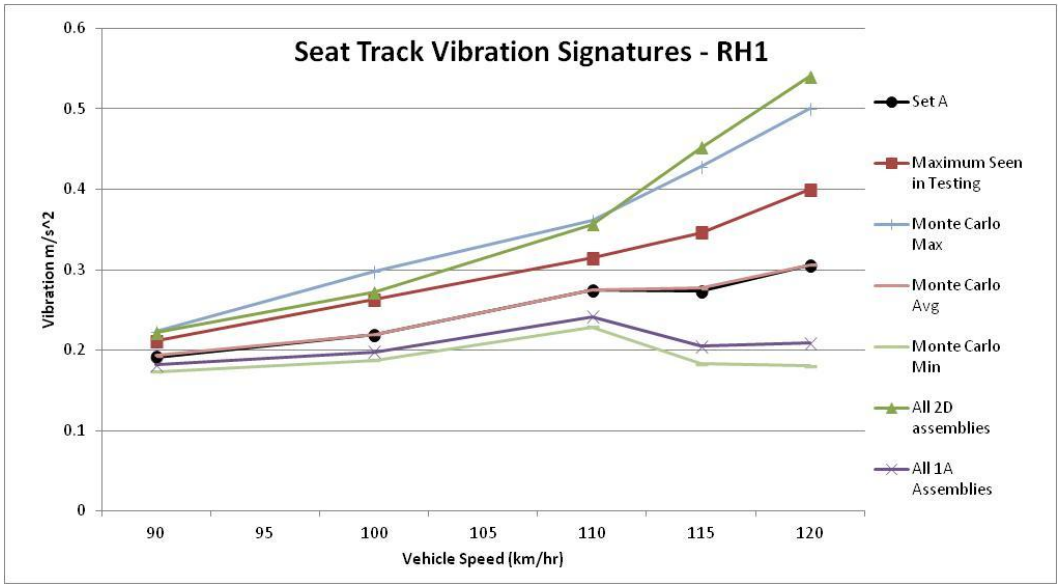

Figure 70 Comparison of Seat Track Vibration Signatures Due to RH1

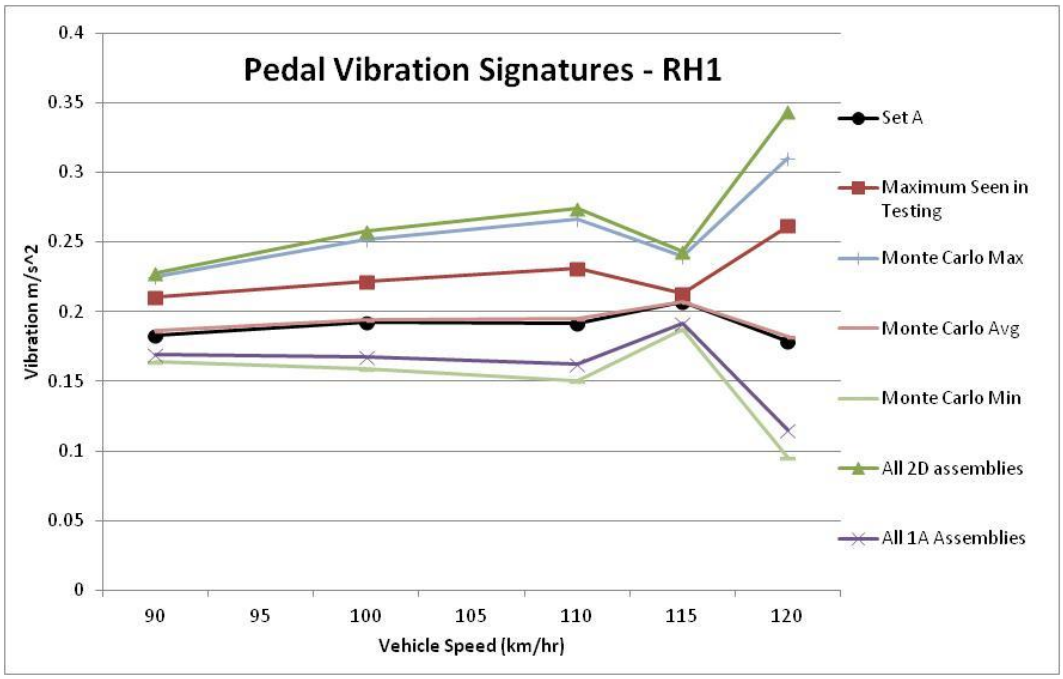

Figure 71 Comparison of Pedal Vibration Signatures Due to RH1

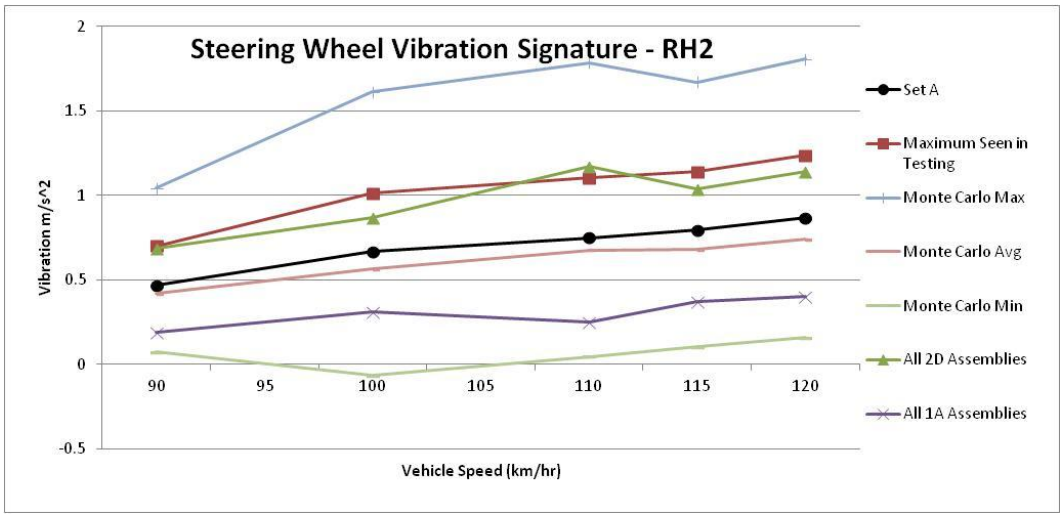

Figure 72 Comparison of Steering Wheel Vibration Signatures Due to RH2

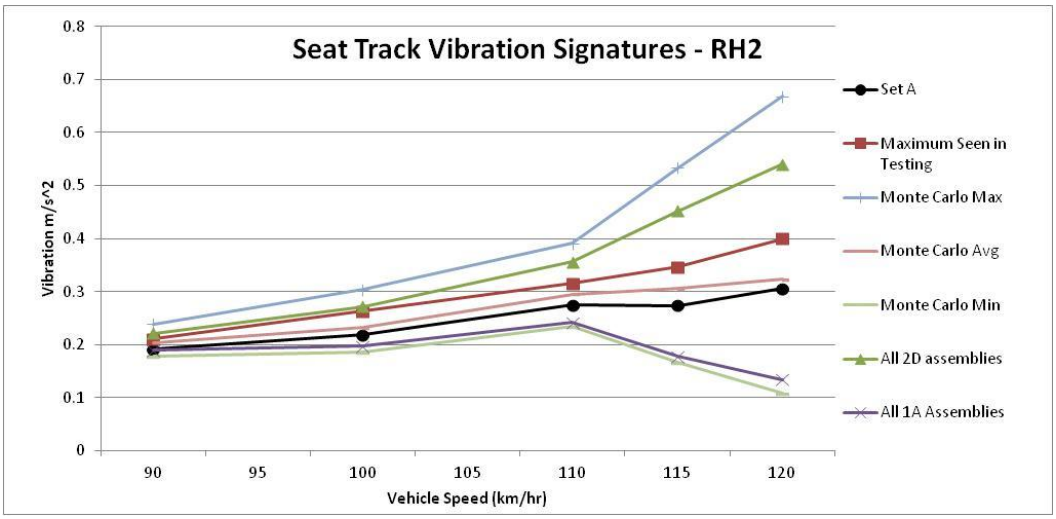

Figure 73 Comparison of Seat Track Vibration Signatures Due to RH2

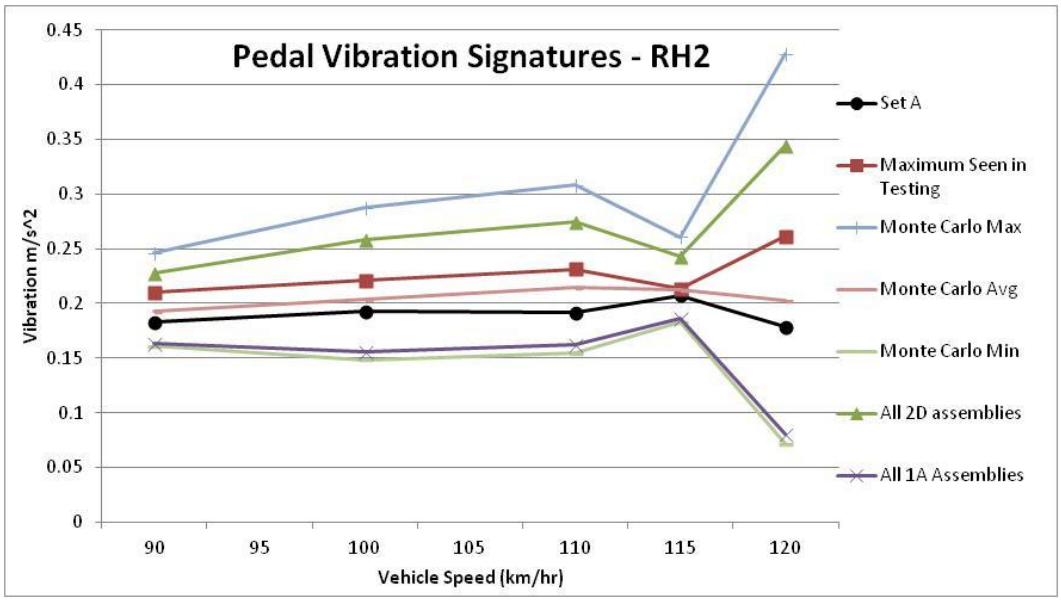

Figure 74 Comparison of Pedal Vibration Signatures Due to RH2

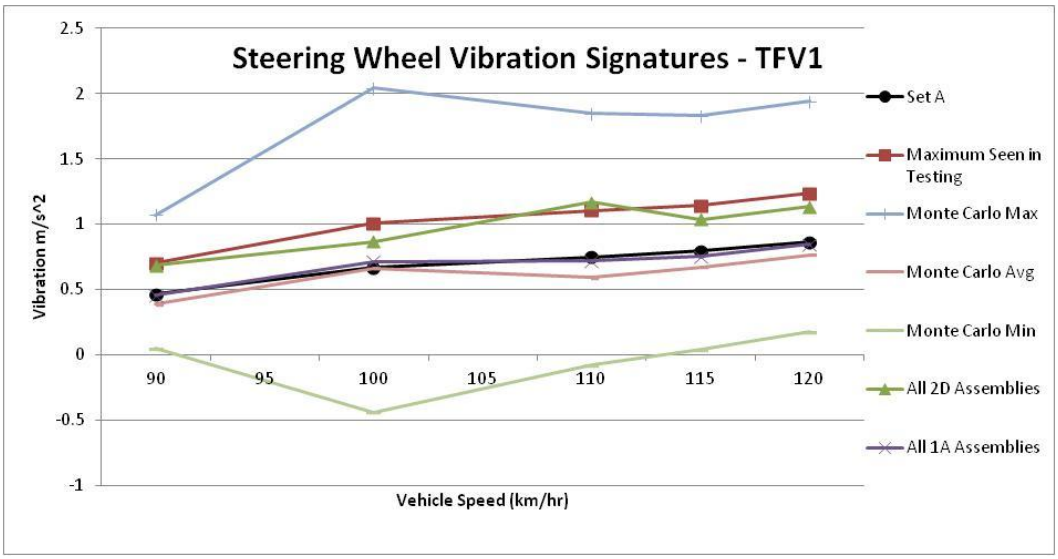

Figure 75 Comparison of Steering Wheel Vibration Signatures Due to TFV1

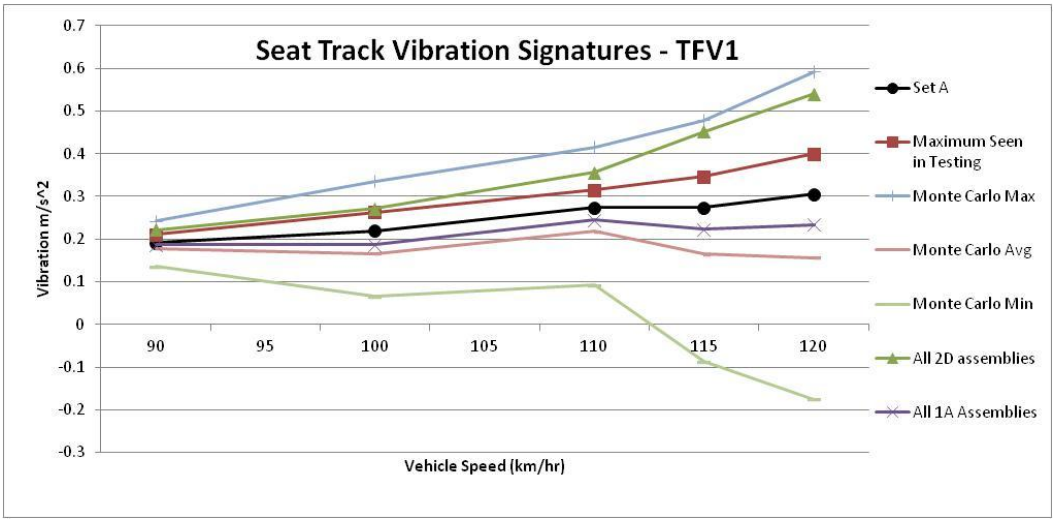

Figure 76 Comparison of Seat Track Vibration Signatures Due to TFV1

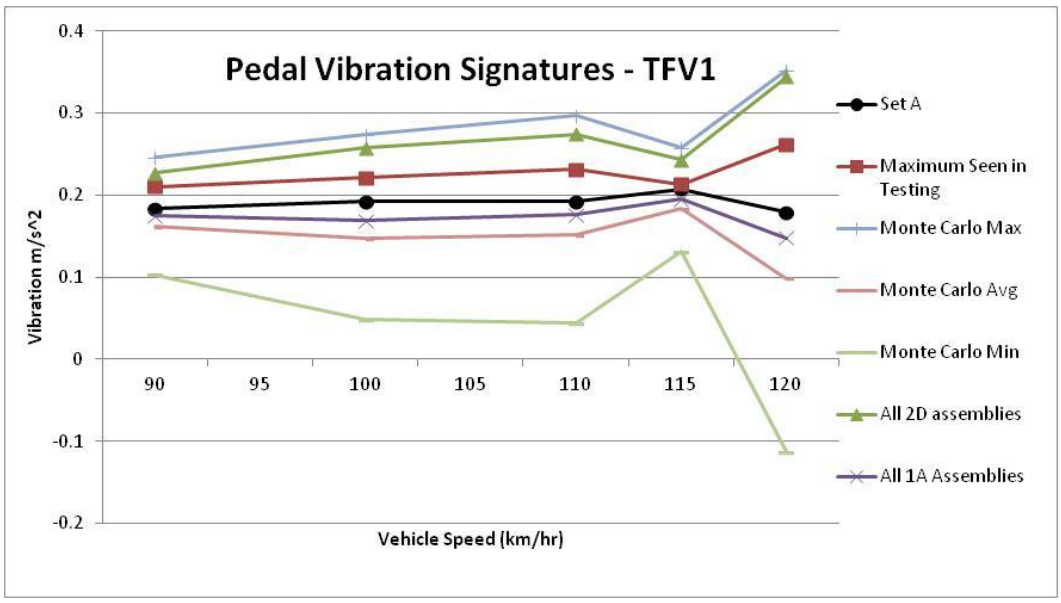

Figure 77 Comparison of Pedal Vibration Signatures Due to TFV1

For the case of TFV2, the assembly with the highest non-uniformity is actually 1A and 2A has the lowest value of TFV2. This can be seen in Figure 21. In the following comparison graphs for TFV2, vibration signatures are predicted for the scenarios that the vehicle is fitted with identical 1A assemblies at all 4 positions for the worst case scenario and identical 2A assemblies at all 4 positions for the best case scenario.

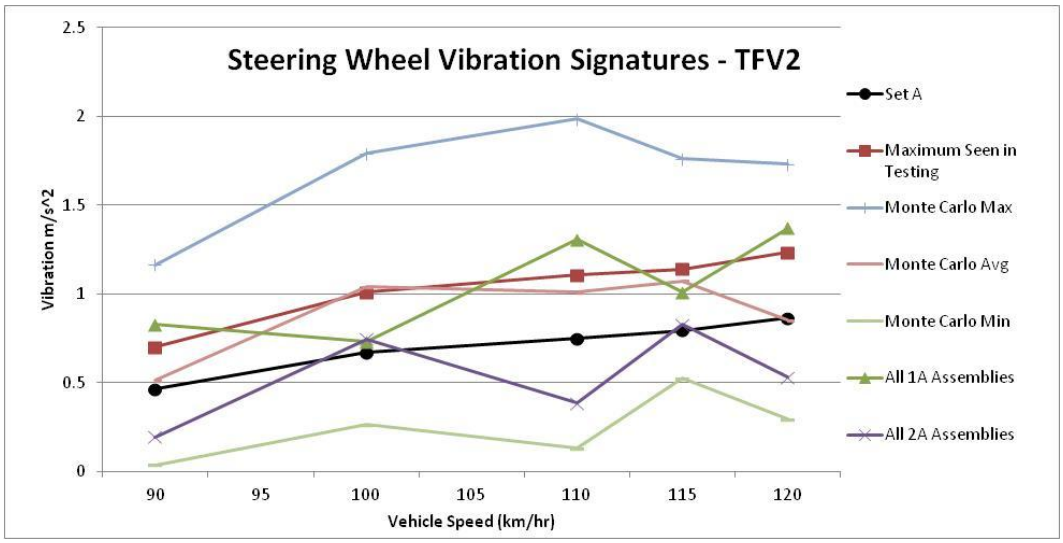

Figure 78 Comparison of Steering Wheel Vibration Signatures Due to TFV2

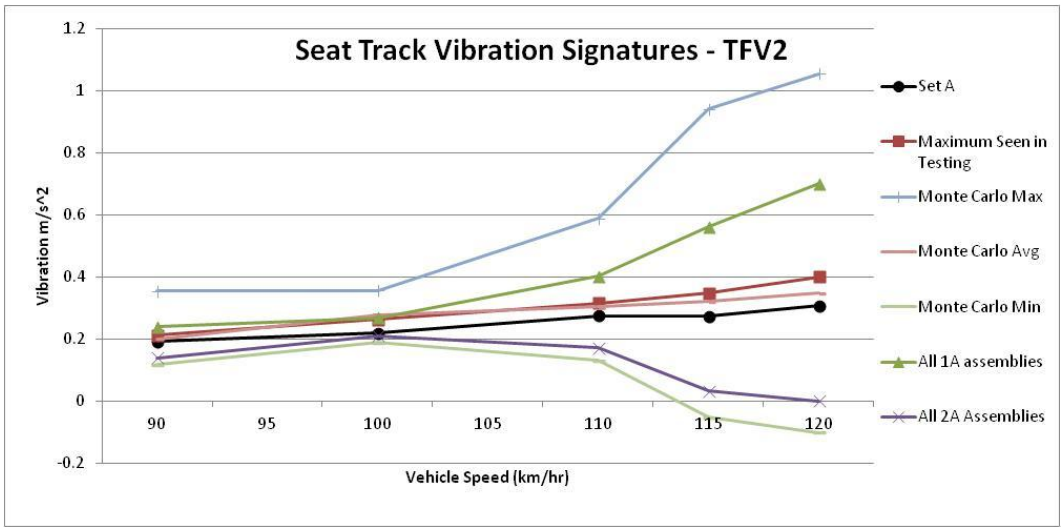

Figure 79 Comparison of Seat Track Vibration Signatures Due to TFV2

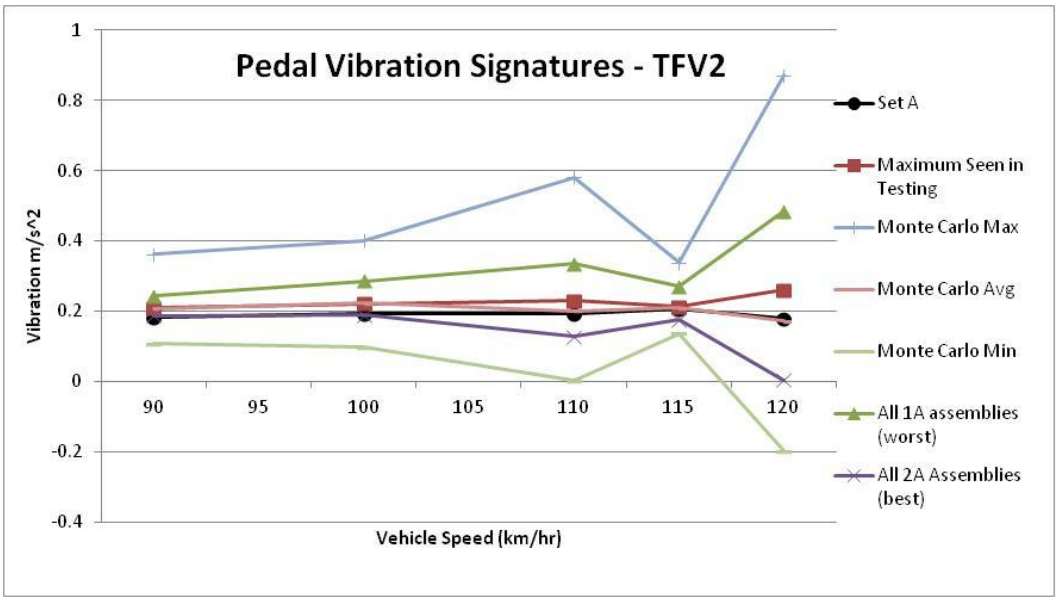

Figure 80 Comparison of Pedal Vibration Signatures Due to TFV2

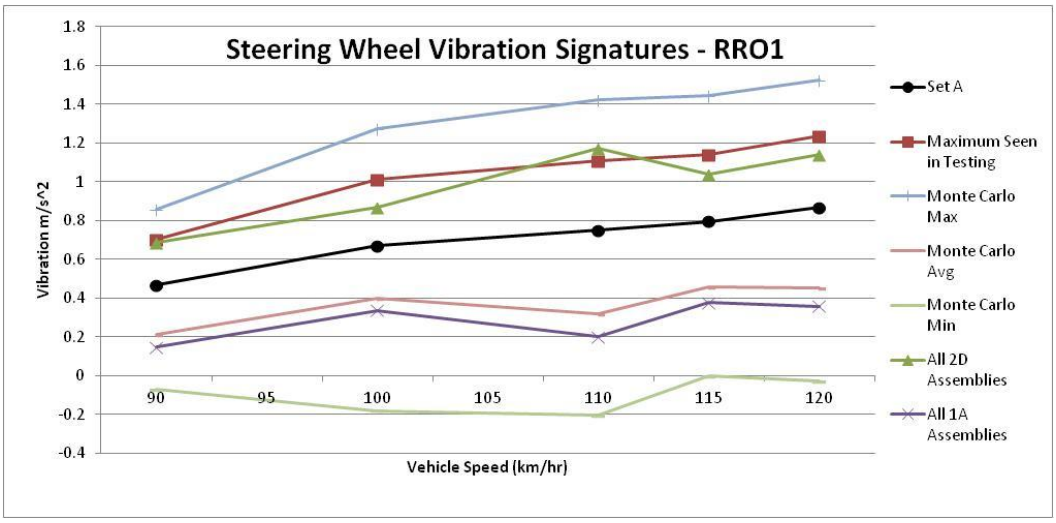

Figure 81 Comparison of Steering Wheel Vibration Signatures Due to RRO1

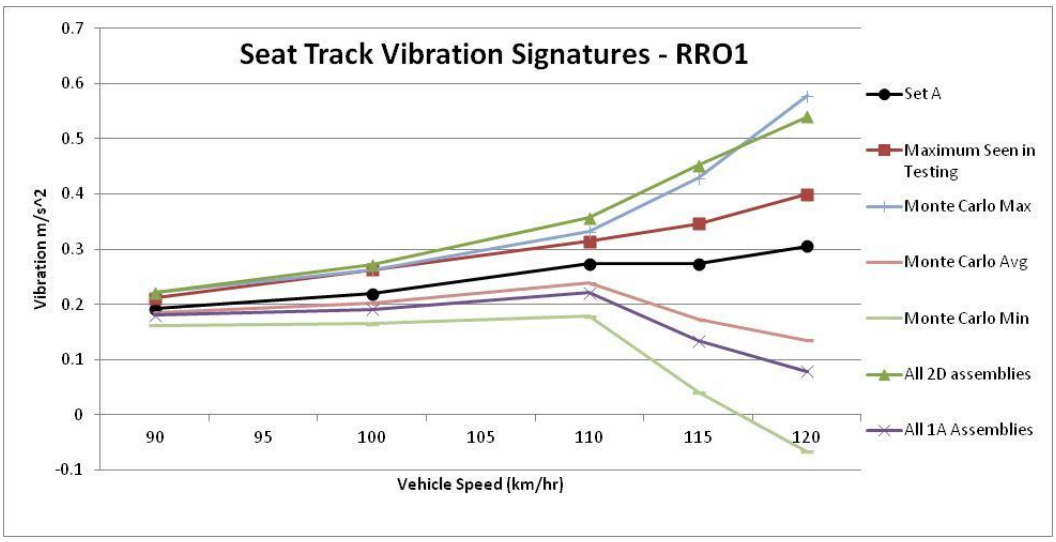

Figure 82 Comparison of Seat Track Vibration Signatures Due to RRO1

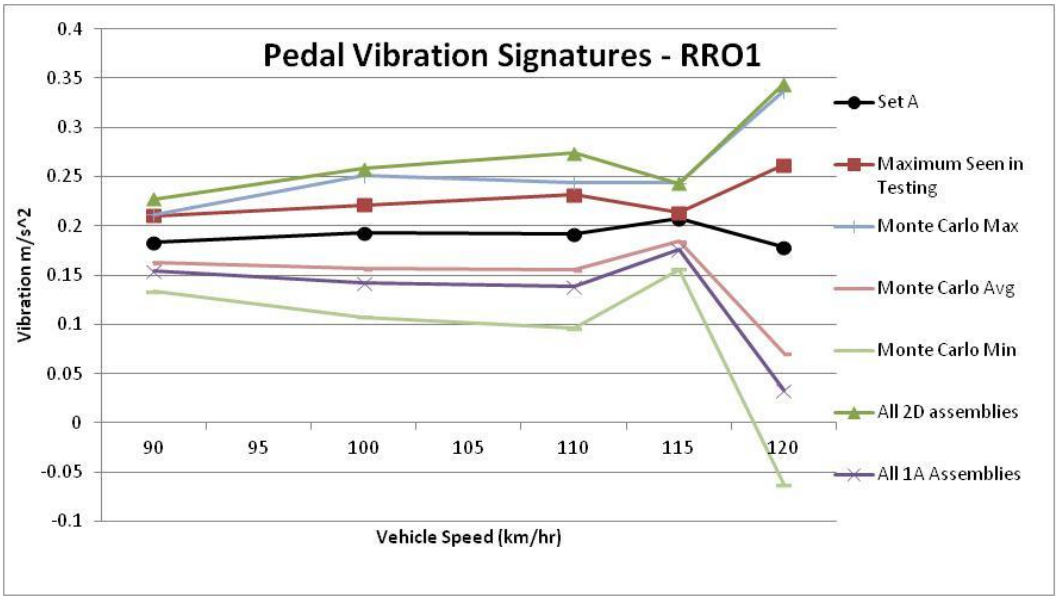

Figure 83 Comparison of Pedal Vibration Signatures Due to RRO1

The relationship between the maximum vibration levels predicted by the Monte Carlo process and the curves to represent three standard deviations can be seen by examining the graphs for each CTP. For this application of the Monte Carlo process in

which 2400 vehicles were simulated, the maximum predicted vibration levels are relatively similar to the 3 standard deviations curve. As previously mentioned, the 99.97% of the data can be expected to fall below the 3 standard deviation line. Therefore, the maximum predicted vibration levels would be approximately the same as the 3 standard deviation curve. If 1 million vehicles were simulated, the maximum predicted vibration levels would most likely be closer to the 6 standard deviation line instead.

Conclusions

The goals of this research were accomplished by providing the design engineer with the tools to determine the most appropriate approach to handle interior vibration levels induced by sources of non-uniformity at the tire/wheel assembly. The process outlined in this research will help design engineers determine how many possible failures can be expected in a batch due to the distribution of non-uniformities at the assemblies. This type of information could be very beneficial for a Six Sigma analysis. An acceptable level of non-uniformity based on targets for interior NVH can also be determined from the process outlined in this research. This research presents a novel type of analysis tool for the identification and analysis of interior NVH response.

Peer Reviewed Publications

- Qatu, .S., King, R., Wheeler, R., Shubailat, O. " e termination of Interior NVH Levels From Tire/Wheel Variations Using a Monte Carlo rocess". Society of Automotive Engineers 011 Noise and ibr ation Conference and Exhibition. Grand Rapids, MI. May 2011. SAE 2011-01-1580

- Qatu, .S., King, R., Shubailat, O., Wheeler, R., " e hicle e sign for Robust Driveline NVH Due to Imbalance and Runout Using a Monte arlo roc ess". Society of Automotive Engineers 011 Noise and Vibration Conference and Exhibition. Grand Rapids, MI. May 2011. SAE 2011-01-1546
- Qatu, .S., King, R., Wheeler, R., Shubailat, O. ebruary 01 . " e hicle Design for Robust Driveline NVH Due to Imbalance and Runout Using a ont e arlo roc ess". *Society of Automotive Engineers International Journal of Passenger Cars – Mechanical Systems*. Volume 4. Issue 1.
- Qatu, .S., Wheeler, R. " etermination of Interior ibration Levels rom Tire/Wheel Assembly Non-Uniformities Using a ont e arlo roc ess". To be submitted.

Future Work

The tire/wheel assemblies to be used for the in-vehicle vibration assessment project need to contain 4 assemblies that have very low values of non-uniformity and 1 assembly that has much higher values of non-uniformity. In reality, the assemblies that were provided for this research did not represent the baseline very well because there was quite a bit of non-uniformity present in some of the Set A assemblies. In addition, assembly 2D did not have dramatically higher non-uniformity properties in all cases. Because of this, there may be errors in the sensitivity curves due to the small change in non-uniformity for some cases. For future projects that use this in-vehicle assessment tool, special attention should be made to select more ideal assemblies in order to obtain more accurate sensitivity curves.

The Set A assemblies had a specific mounting location on the vehicle and those locations did not vary. For example, if assembly 1A was mounted on the vehicle, it was always in the front driver position. However, if the Set A assemblies are rotated to different positions on the vehicle and vibration signatures are acquired, multiple sensitivity curves for each assembly position can be determined. This can aid in determining sensitivity curves that better represent a sample of vehicles as well as eliminating some of the uncertainty involved in the sensitivity calculations. Similarly, if the process were repeated with another assembly in the place of 2D, 2 sensitivity curves can be determined instead of just one. This would eliminate some of the error involved in the sensitivity calculations, and the sensitivity function may be found to be nonlinear if this process were continued.

Further work should be done with this project in order to better understand the effect of measurement error throughout the project. Multiple test runs, with different drivers, on different road areas need to be compared. The effect of the mounting positions of the accelerometers should also be examined.

Another direction of future work could be to study the effects of phasing. Phasing refers to the interaction between the high and low spots of each assembly. Some phase interactions were witnessed during the 300 second test runs, but might not have occurred between the same axle assemblies. However, these interactions can be forced by rotating the assemblies around the wheel hub. For example, acquire a baseline vibration signature from the vehicle with all 4 Set A assemblies. Then, rotate the front passenger assembly around the hub and rerun the test. Compare the vibration signatures and see if any phase interactions were witnessed that either improved the vibration signature or caused higher

vibration levels. This process can be repeated at all 4 assembly positions and again while rotating the 2D assembly to each position on the vehicle. This research could go even further to then bring imbalance into the analysis. If the high and low spots of imbalance and force variations are known, and the mounting angle of the assembly is varied, it might be possible to find relationships between imbalance and various force variations. For example, there may be instances in which mounting a certain amount of imbalance at a certain mounting angle compared to another assembly could lead to a reduction of driver-felt vibrations due to a certain force variation. In effect, understanding the phase interactions and relationships of assemblies and their mounting angles may reduce the amount of driver-felt vibrations.

REFERENCES

1. P. Gu and M. McKee. An Innovative Method of Simulating Tire Non-Uniformity Forces for Vehicle Vibration Sensitivity Measurements. SAE Transactions 2009-01-2086, 2009.

2. M. Hashioka and I. Kido. An Application Technique of Transfer Path Analysis for Automotive Body ibra tion," SAE Transaction 2007-01-2334.

3. ottinger, .G ., "Uniformity: A ruc ial Attribute of Tire/Wheel Assemblies," Tire Science and Technology, TSTCA, Vol. 38, No. 1, January-March 2010, pp. 24-46.

. or fi, H.R., "Tire Non-Uniformities and Steering Wheel ibr ations," Tire Science and Technology, TSTCA, Vol. 33, No. 2, April-June 2005, pp. 64-102.

5. Schuring, .J ., "Uniformity of Tire-Wheel Assemblies," Tire Science and Technology, TSTCA, Vol. 19, No. 4, October-December 1991, pp.213-236.

6. Zheglov, A., "How to Match to Weibull ist ribution in Excel," http://learningagileandlean.wordpress.com/2013/08/01/how-to-match-to-weibull-distribution-in-excel/

7. Wittwer, J.W., "Generating Random Numbers in Excel for Monte Carlo Simulation" From Vertex42.com, June 1, 2004, http://www.vertex42.com/ExcelArticles/mc/GeneratingRandomInputs.html

8. Nissan, "Shake Shimmy Testing," 011.

9. Qatu, MS, and M. H. Sirafi. Robustness of Powertrain Mount System for Noise, Vibration and Harshness at Idle," Journal of Automobile Engineering, 216, 805-810, 2002.

10. M.H. Sirafi, M.H and M.S. Qatu. Robustness of mount systems for idle NVH, part I: centre of gravity (cg) mounts" Int. J. of vehicle noise and Vibration, 2 (4), 317-333, 2006.

11. M.H. Sirafi, M.H. and M.S. Qatu, " Robustness of Mount Systems for Idle NVH, part II: Pendulum Mounts" Int. J. of Vehicle Noise and Vibration, Vol 2 (4), pp. 334-340, 2006.

12. M.H. Sirafi, and M.S. Qatu, "Accurate Modeling for the Powertrain and Subframe Modes", SAE Transactions No. 2003-01-1469, Proceedings of 2003 Noise and Vibration Conference, Traverse City, Michigan, May 2003.

13. M.S. Qatu, and J. Iqbal, "Robustness of Axle Mounts System for Driveline NVH," SAE Transactions No. 2003-01-1485, Proceedings of 2003 Noise and Vibration Conference, Traverse City, Michigan, May 2003.

14. J. Pang, and M.S. Qatu, "Exhaust System Robustness Analysis Due to Flex Decoupler Stiffness Variation," SAE Transactions No. 2003-01-1649, Proceedings of 2003 Noise and Vibration Conference, Traverse City, Michigan, May 2003

15. M.S. Qatu, M.K., Abdelhamid, J Pang, and G. Sheng, Overview of Automotive Noise and Vibration. Int. J. Vehicle Noise and Vibration, 5 (1/2), 1-35, 2009.

16. J. Park, M. McKee and T. Mouch. Experimental Estimation of On-Vehicle Wheel-End Force and Application to Tire Flat-Spotting Effect. SAE Transactions 2009-01-2160, 2009.

17. N. Tsujiuchi, T. Koizumi , . atsuba ra , K. orig uchi and I. Shima. " rediction of Spindle orce Using easured Road orces on Rolling Tire." SAE Transactions 2009-01-2107.

18. E-U Saemann, . R opers, J. orkholt, A. Omr ani, "Identification of Tire ibra tions," SAE Transactions 003 -01-1528.

19. Song, S., ak, . Hong, S., Oh, J., Kim, J., and Kim, . " ibra tion Analysis of the Steering Wheel of a Passenger Car Due to the Tire Non-Uniformity." SAE 931918.

20. Kim, K. Park, J. and Lee, S., "Tire ass Imbalance, Rolling hase iff erence, Non-Uniformity Induced Force Difference, an Inflation Pressure Change Effects on Steering Wheel ib ration", SAE 005-01-2317.

1. B oulahbal, ., ankau, J., and Gauterin, ., "Sensitivity of Steering Wheel Nibble to Suspension arameters, Tire ynamics, and Brake Judder", SAE 005-01-2316.

. Gu, ., cK ee, ., S tone, K., and Wiley, R., " e vices and ethods for Simulating Tire Non-Uniformity Forces for Vehicle Vibration Sensitivity Measurements and Tuning," U.S atent No. 7100 3 .

3. ark, J., Gu, ., cK ee, ., a nd ouch , T., "Empirical e termination of On-Vehicle Wheel-End orces", I A , eb. 19-22, 2007, Orlando, Florida.

24. M. Hashioka and I. Kido. An Application Technique of Transfer Path Analysis for Automotive Body ibra tion," SAE Transaction 007 -01-2334.

5. or ner, W. ., “ Using i crosoft Excel for Weibull Analysis,” 1999, http://www.qualitydigest.com/magazine/1999/jan/article/using-microsoft-excel-weibull-analysis.html